

# Experimental results of the SPIDER negative ion accelerator in view of the next operations

E Sartori<sup>1,2</sup>, R. Agnello<sup>1,3</sup>, M. Agostini<sup>1</sup>, M. Barbisan<sup>1</sup>, M. Bigi<sup>1</sup>, M. Boldrin<sup>1</sup>, M. Brombin<sup>1</sup>, V. Candeloro<sup>1,2</sup>, R. Casagrande<sup>1</sup>, S. Dal Bello<sup>1</sup>, M. Dan<sup>1</sup>, B.P. Duteil<sup>1,3</sup>, M. Fadone<sup>1</sup>, L. Grandò<sup>1</sup>, P. Jain<sup>1</sup>, A. Maistrello<sup>1</sup>, I. Mario<sup>1,6</sup>, R. Pasqualotto<sup>1</sup>, M. Pavei<sup>1</sup>, A. Pimazzoni<sup>1</sup>, C. Poggi<sup>1</sup>, A. Rizzolo<sup>1</sup>, A. Shepherd<sup>1,4</sup>, M. Ugoletti<sup>1</sup>, P. Veltri<sup>5</sup>, B. Zaniol<sup>1</sup>, P. Agostinetti<sup>1</sup>, D. Aprile<sup>1</sup>, G. Berton<sup>1</sup>, C. Cavallini<sup>1</sup>, M. Cavenago<sup>6</sup>, G. Chitarin<sup>1,2</sup>, G. Croci<sup>7</sup>, R. Delogu<sup>1</sup>, M. De Muri<sup>1</sup>, M. De Nardi<sup>1,2</sup>, S. Denizeau<sup>1</sup>, F. Fellin<sup>1</sup>, A. Ferro<sup>1</sup>, E. Gaio<sup>1</sup>, C. Gasparini<sup>1</sup>, A. Luchetta<sup>1</sup>, F. Lunardon<sup>1,2</sup>, G. Manduchi<sup>1</sup>, N. Marconato<sup>1,2</sup>, D. Marcuzzi<sup>1</sup>, O. McCormack<sup>7</sup>, R. Milazzo<sup>1</sup>, A. Muraro<sup>8</sup>, T. Patton<sup>1</sup>, N. Pilan<sup>1</sup>, M. Recchia<sup>1</sup>, A. Rigoni-Garola<sup>1</sup>, F. Santoro<sup>1,2</sup>, B. Segalini<sup>1,2</sup>, M. Siragusa<sup>1</sup>, M. Spolaore<sup>1</sup>, C. Taliercio<sup>1</sup>, V. Toigo<sup>1</sup>, P. Veltri<sup>5</sup>, P. Zaccaria<sup>1</sup>, R. Zagorski<sup>1,9</sup>, L. Zanutto<sup>1</sup>, M. Zaupa<sup>1</sup>, M. Zuin<sup>1</sup>, G. Serianni<sup>1</sup>

<sup>1</sup>Consorzio RFX, Corso Stati Uniti 4, I-351, 27 Padova, Italy

<sup>2</sup> Department of Management and Engineering, Università degli Studi di Padova, Strad. S. Nicola 3, 36100 Vicenza, Italy

<sup>3</sup> Ecole Polytechnique Fédérale de Lausanne (EPFL) - Swiss Plasma Center (SPC), 1015 Lausanne, Switzerland

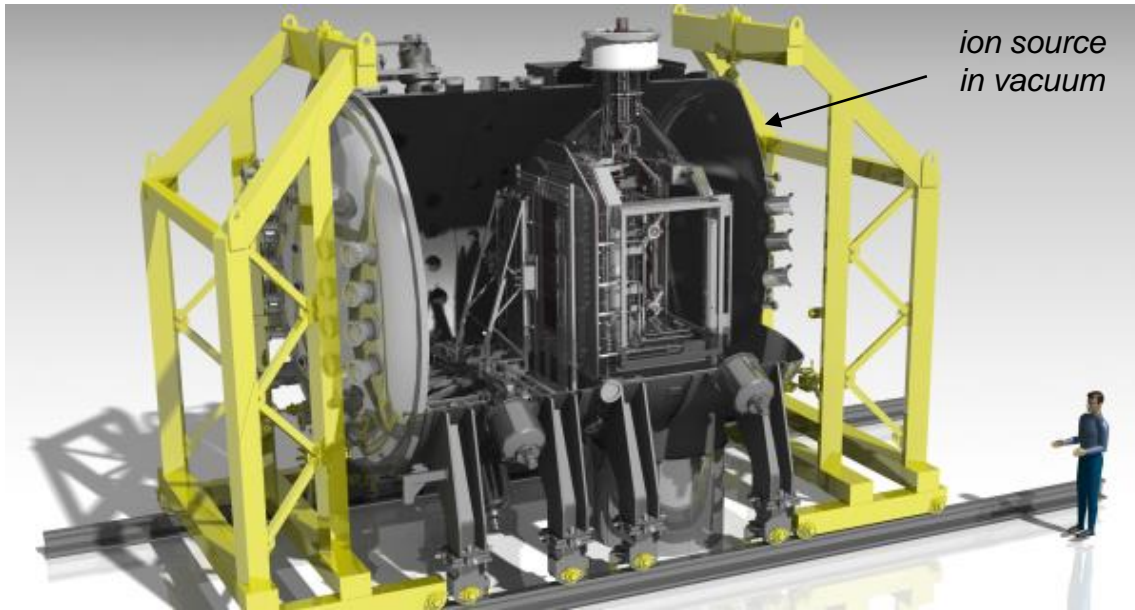
<sup>4</sup>CCFE, Culham Science Centre, Abingdon OX14 3DB, Oxon, UK

<sup>5</sup>ITER Organization (IO), Route de Vinon sur Verdon, CS 90 046, F-1, 3067 St. Paul-lez-Durance, France

<sup>6</sup>Istituto Nazionale Fisica Nucleare, Italy

<sup>7</sup> National Centre for Nuclear Research (NCBJ), PL-05-400 Otwock, Poland

# SPIDER full-size prototype source for ITER HNB



Full scale **plasma source** of ITER Heating Neutral Beams;  
RF plasma source based on IPP design, 2x ELISE

Targets: optimisation of

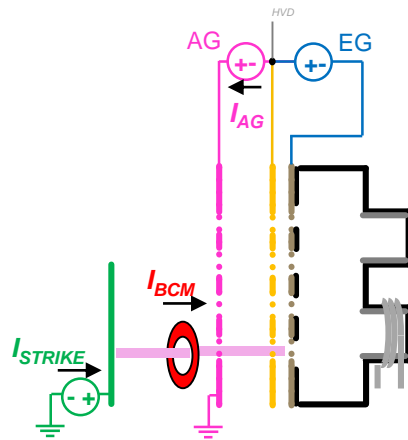
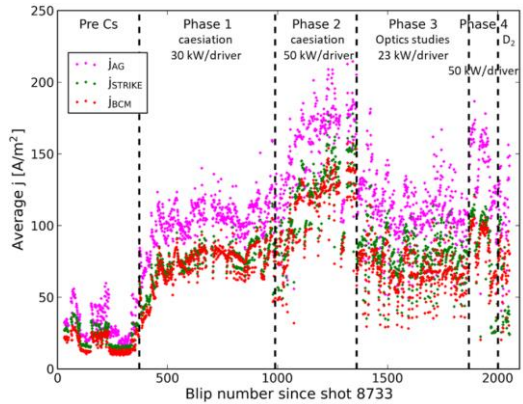
- Extracted current density ( $355 \text{ A/m}^2 \text{ H}^-$ ,  $285 \text{ A/m}^2 \text{ D}^-$ )
- Uniformity over 1280 apertures (within 10%)
- Stability (1 h beam)
- Co-extracted electron fraction ( $<0.5 \text{ H}^-$ ,  $<1 \text{ D}^-$ )

- 2018 *first plasma*
- influence of vessel pressure on RF discharges clarified*
- 2019 *first extracted beam, masking most extraction apertures*
- source plasma studied with movable probes*
- 2020 *Improving availability and reliability [1h/day plasma on]*
- HV >30kV available*
- First operation with caesium*
- 2021 *shutdown for improvements*

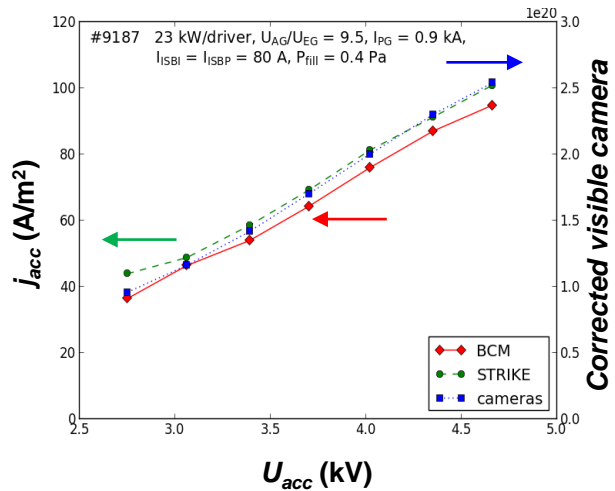
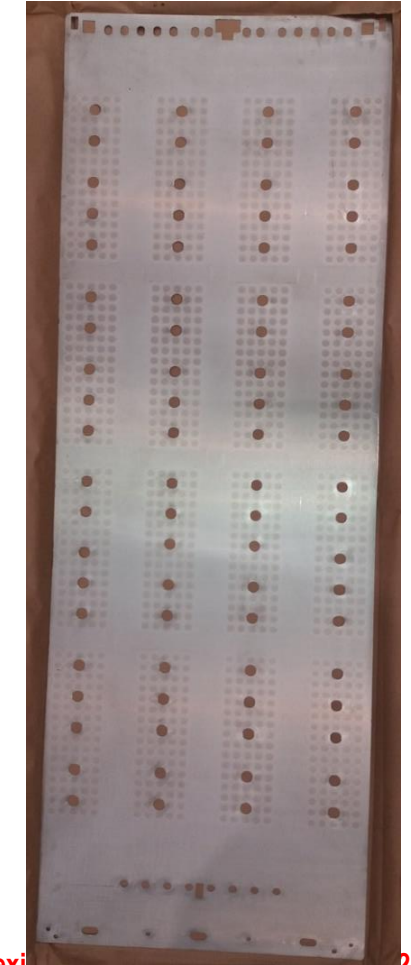
**AIM OF THIS PRESENTATION:**  
Discuss how to improve SPIDER beam parameters using experimental results obtained so far

- Measuring beam current and improvements
- Vertical profile of beam current
- Vertical profile of plasma parameters
- Operation of caesium ovens
- Non-homogeneity among RF drivers: vertical and horizontal
- Transverse field inside drivers and RF coupling
- New needs for plasma source diagnostics
- Reducing beamlet core divergence
- Operating full-size ITER HNB prototype source with 1280 apertures

# Measurement of negative ion beam current



- Measurement of negative-ion beam current not straightforward: experience with single-beamlets [1] extremely useful as «training» in view of next op. without PG mask
- beam current <80% acceleration current from HV power supply
- Indications for future operation from frequency analysis of accelerated current:



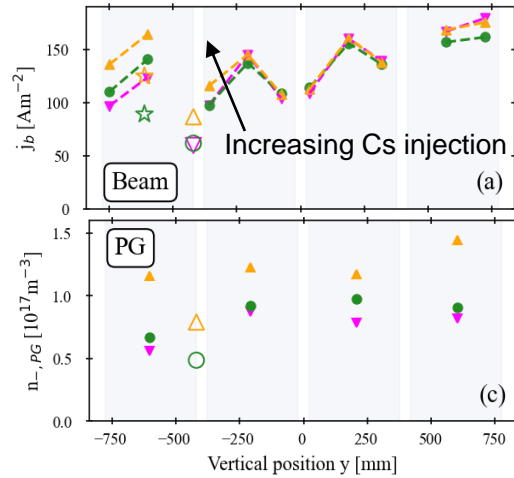
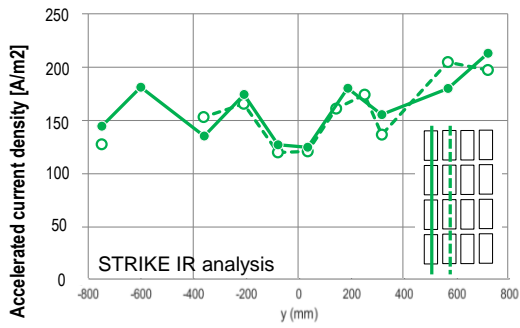
FREQUENCY ANALYSIS OF ACCELERATED BEAM CURRENT[2]

Frequency range	Cause	$I_R$ [%] (M & Bz)	$I_R$ [%] (F)
0.9 - 1.1 MHz	Driver oscillators	1 - 5%	5 - 15%
0.8 - 2 kHz	Driver beatings	< 2%	< 2%
Nx50 Hz	Power supplies	1 - 7%	1 - 10%
~ 140 kHz	EG power supply	0.5 - 6%	0.5 - 10%

[1] S Alastair, Direct current measurements of the SPIDER beam: a comparison to existing beam diagnostics, NBS 2022

[2] B. Pouradier-Duteil, First characterization of the SPIDER beam AC component with the BeamletCurrent Monitor, SOFT 2022

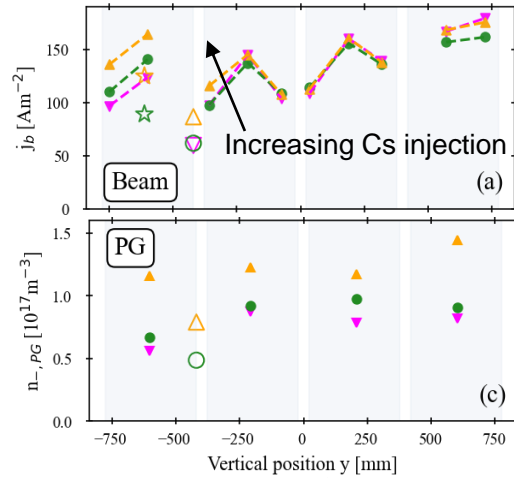
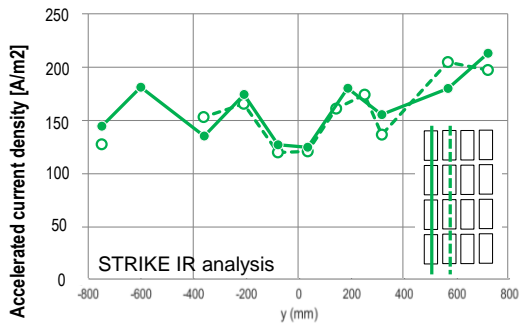
# Measurement of negative ion beam current profile



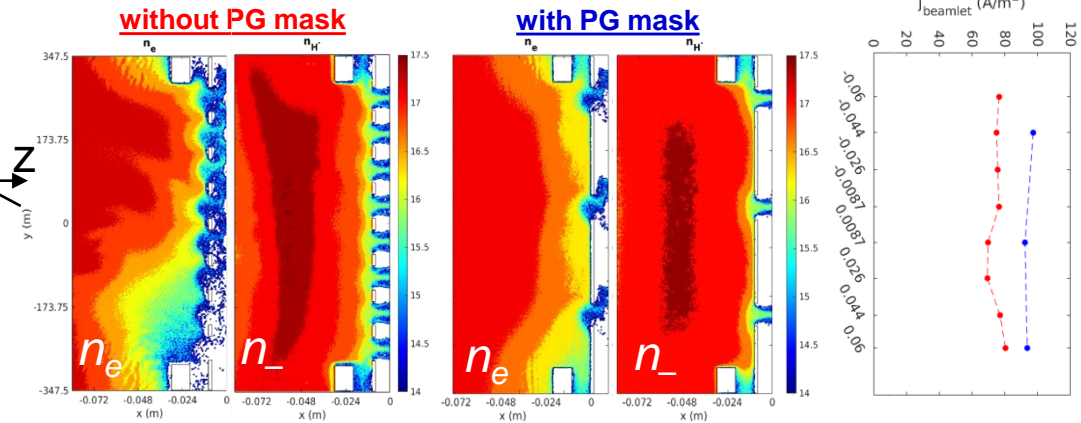
- Not-so-uniform vertical profile, even within each beamlet group<sup>[1,2]</sup>: possible to measure only thanks to PG mask covering most apertures (individual beamlets)

[1] E Sartori, First operations with caesium of the negative ion source SPIDER, Nucl. Fusion 62 086022 (2022)  
[2] G. Serianni, Spatially resolved diagnostics for optimization of large ion beam sources, RSI 93 (8), 081101 (2022)

# Measurement of negative ion beam current profile

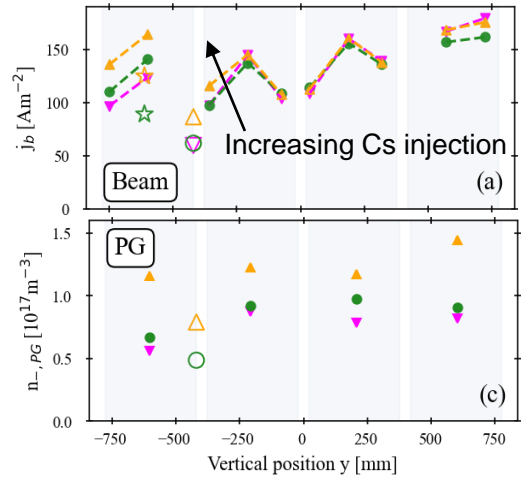
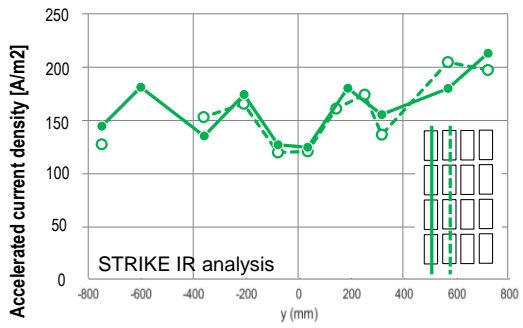


- Not-so-uniform vertical profile, even within each beamlet group<sup>[1,2]</sup>: possible to measure only thanks to PG mask covering most apertures (individual beamlets)
- Study of extraction region 2D PIC: uniform flux from plasma side, rather uniform H<sup>-</sup> beamlets extracted. Masking does not modify spatial distribution of  $n_-$ , only increases absolute value<sup>[3]</sup>

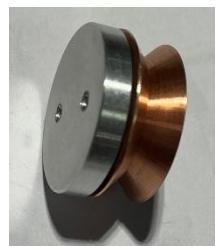
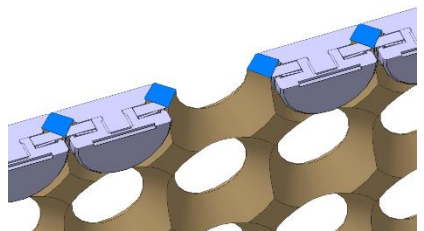
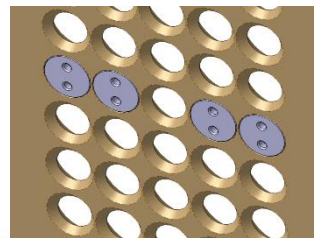
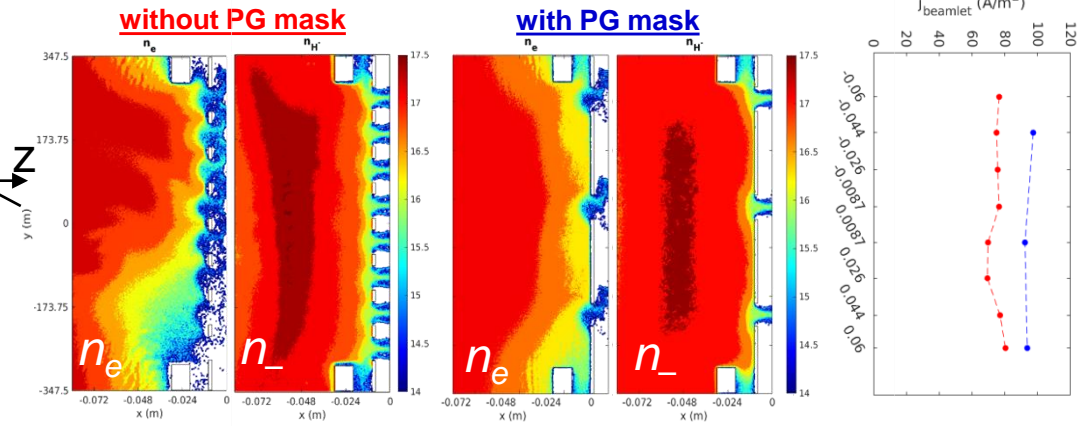


[1] E Sartori, First operations with caesium of the negative ion source SPIDER, Nucl. Fusion 62 086022 (2022)  
 [2] G. Serianni, Spatially resolved diagnostics for optimization of large ion beam sources, RSI 93 (8), 081101 (2022)  
 [3] E Sartori, Influence of plasma grid-masking on the results of early SPIDER operation, SOFT 2022

# Measurement of negative ion beam current profile

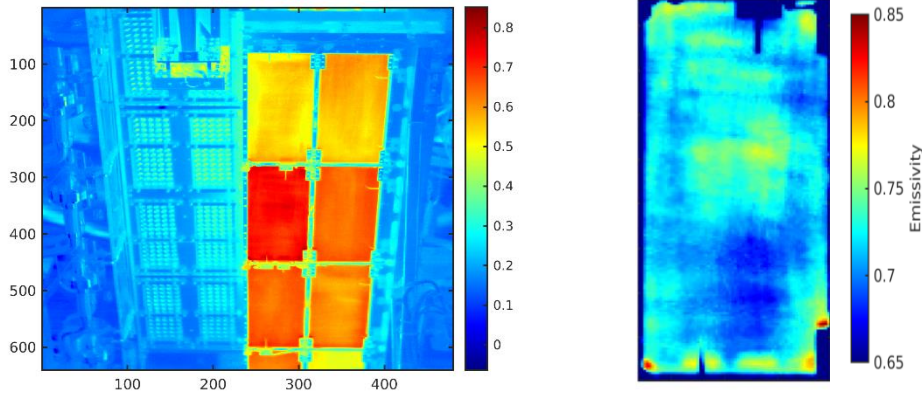


- Not-so-uniform vertical profile, even within each beamlet group<sup>[1,2]</sup>: possible to measure only thanks to PG mask covering most apertures (individual beamlets)
- Study of extraction region 2D PIC: uniform flux from plasma side, rather uniform H<sup>-</sup> beamlets extracted. Masking does not modify spatial distribution of n<sub>-</sub>, only increases absolute value<sup>[3]</sup>
- Single beamlet studies proposed also for future operation: uniformity within the beamlet group, operation of Allison Emittance Scanner<sup>[4]</sup>

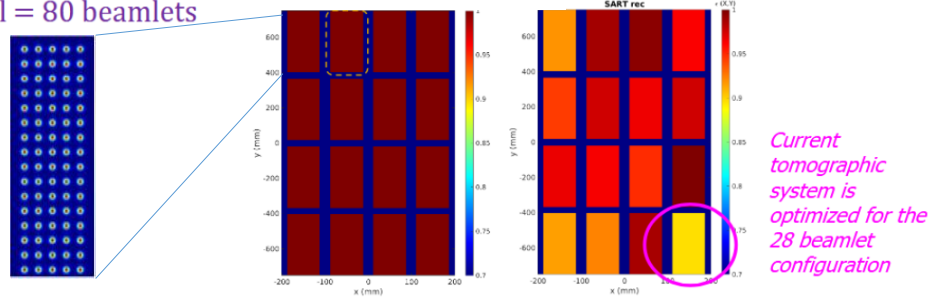


[1] E Sartori, First operations with caesium of the negative ion source SPIDER, Nucl. Fusion 62 086022 (2022)  
 [2] G. Serianni, Spatially resolved diagnostics for optimization of large ion beam sources, RSI 93 (8), 081101 (2022)  
 [3] E Sartori, Influence of plasma grid-masking on the results of early SPIDER operation, SOFT 2022  
 [4] C Poggi, First tests and commissioning of the emittance scanner for SPIDER, FED 168, 112659 2021

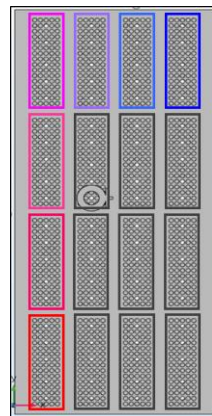
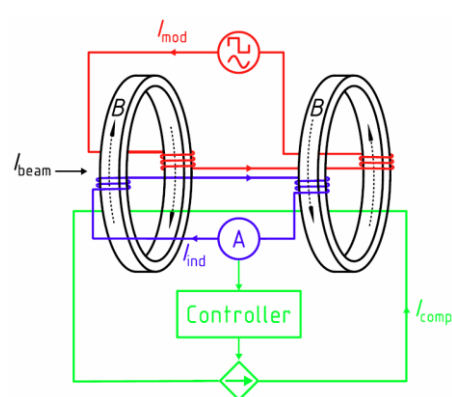
# Measurement of negative ion beam current profiles



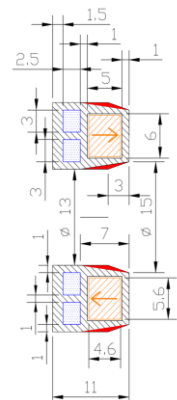
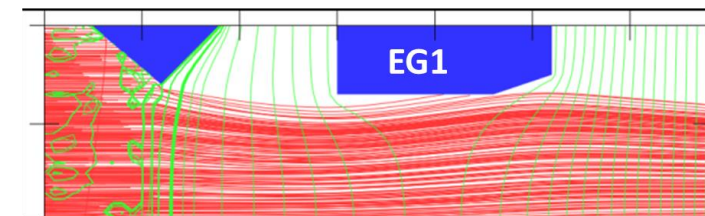
1 pixel = 80 beamlets



- Preparation of 2D correction maps of CFC emissivity to improve accuracy of STRIKE diagnostic calorimeter
- Preparation of beam tomography from visible cameras [1]
- Feasibility study to develop «beamlet group current monitors» [2] based on fluxgate concept (Direct Current Current Transformer)
- Machining tapering of EG aperture to reduce beamlet intercetion: maximise the experimental window with full beam transmission is important to correctly measure the non uniformities



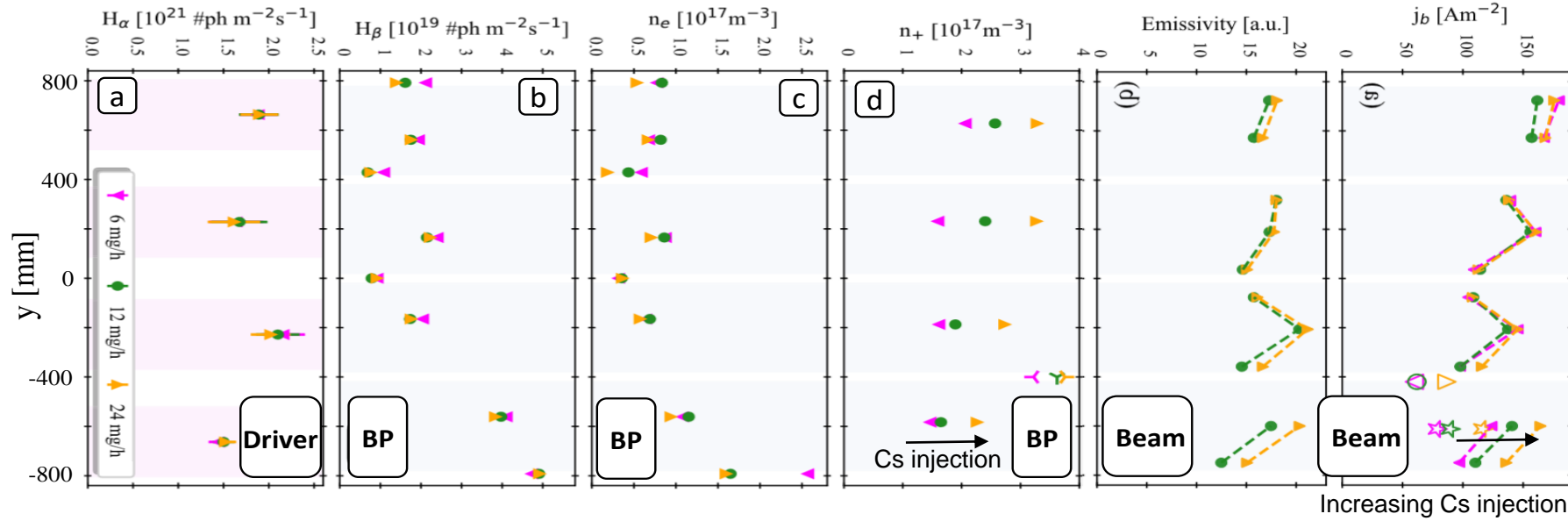
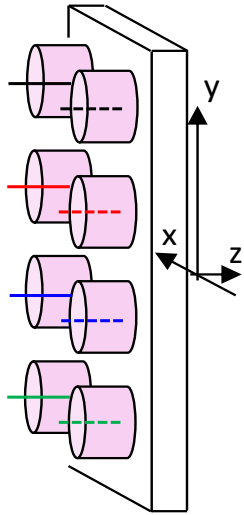
H-, J=380 A/m<sup>2</sup> VEG=9.4 kV VGG=100 kV (APGS=90.6 kV)



[1] M Ugoletti, Development of the tomographic reconstruction technique of SPIDER negative ion beam, SOFT 2022  
 [2] R Pasqualotto, Improvement of SPIDER diagnostic systems, SOFT 2022

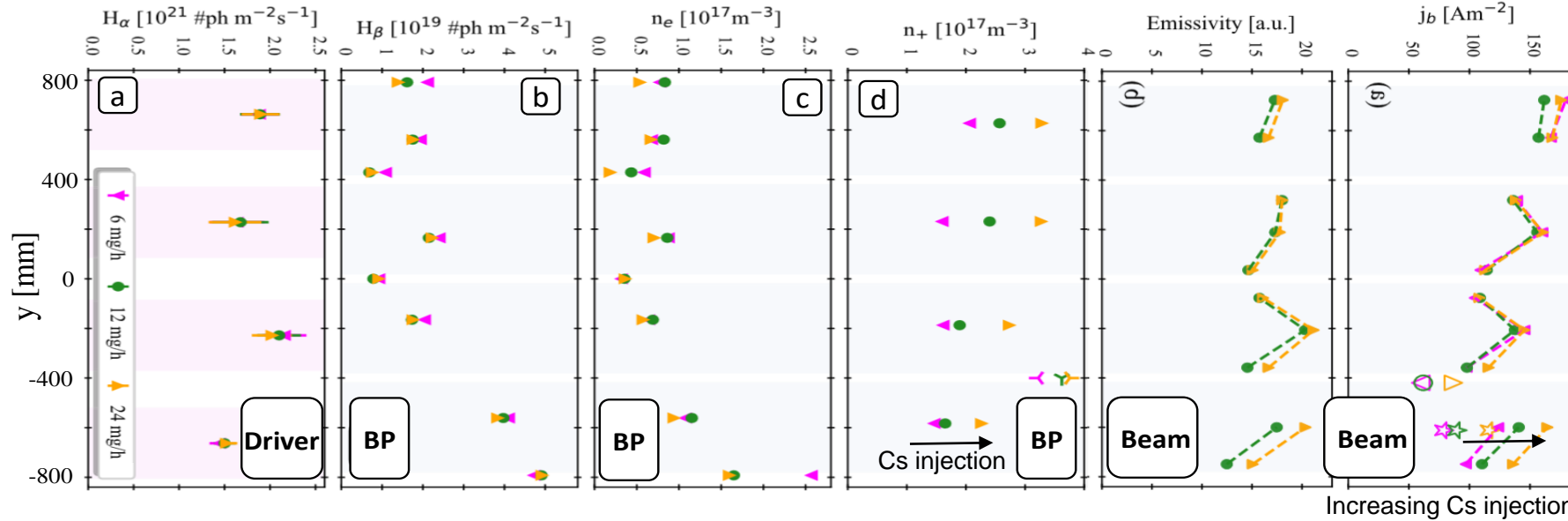
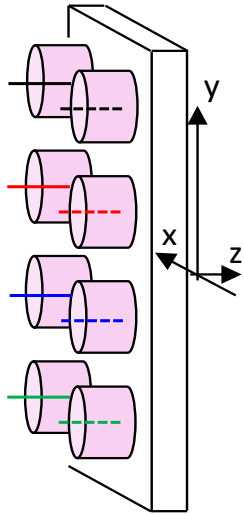


# Plasma parameters and beamlet current profile

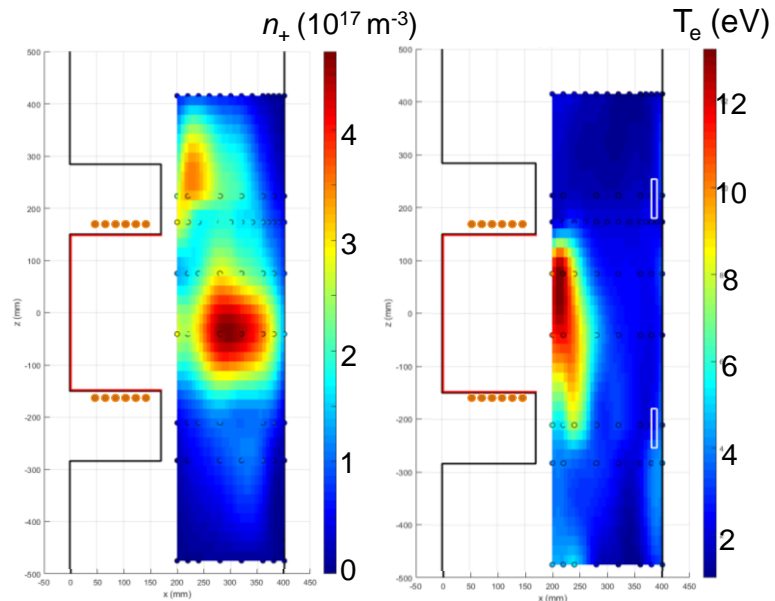


- Plasma parameters inside drivers appear to be uneven

# Plasma parameters and beamlet current profile



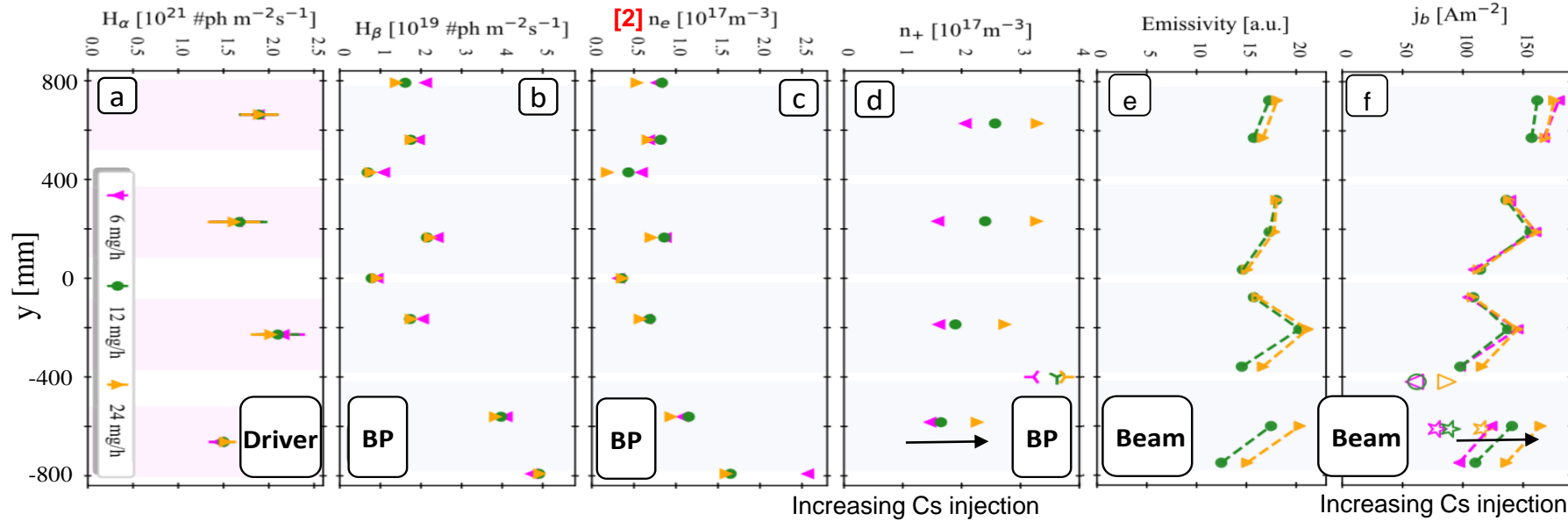
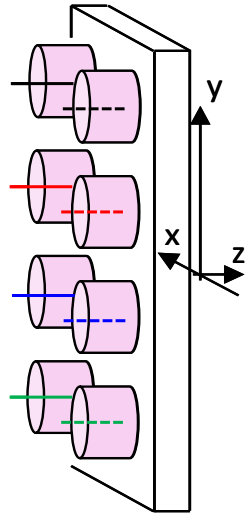
PREVIOUS MEASUREMENT WITH MOVABLE ELECTROSTATIC PROBES



- Plasma parameters inside drivers appear to be uneven
- At the bottom of the source, electrons reach the extraction region; flow of hot electrons from drivers; caesium does not affect this drift

[1] G Serianni, Spatially resolved diagnostics for optimization of large ion beam sources, RSI 93 (8), 081101 (2022)

# Plasma parameters and beamlet current profile

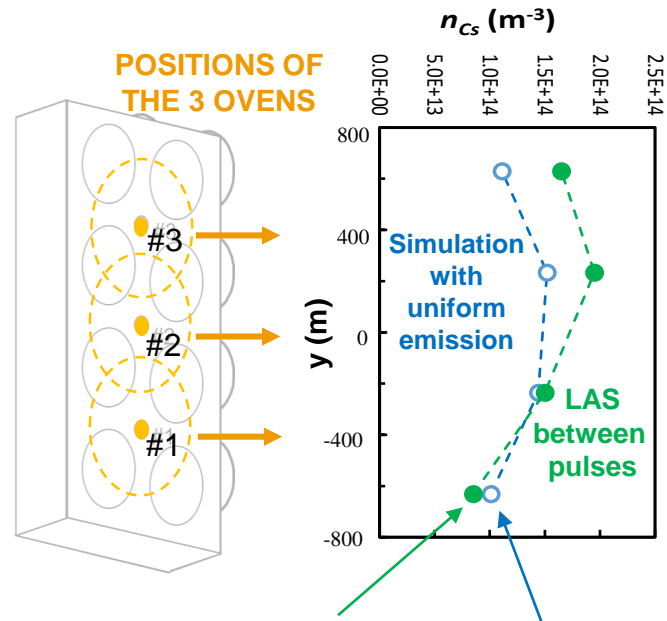


- Plasma parameters inside drivers appear to be uneven
- At the bottom of the source, electrons reach the extraction region; flow of hot electrons from drivers; caesium does not affect this drift
- At the bottom, less positive ions; less beamlet current; caesium evaporation improves both
- Visual inspection: PG/BP surface clean at the bottom

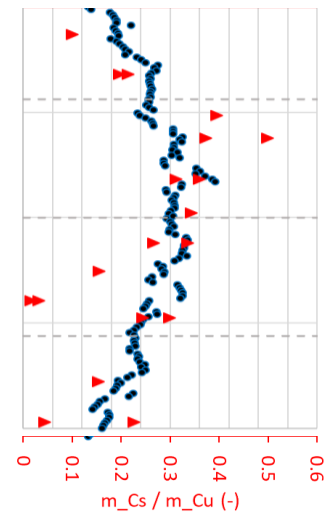
[1] G Serianni, Spatially resolved diagnostics for optimization of large ion beam sources, RSI 93 (8), 081101 (2022)

[2] B Pouradier Duteil, Characterization of the Plasma in SPIDER using a Cs-H Collisional Radiative model, NIBS 2022

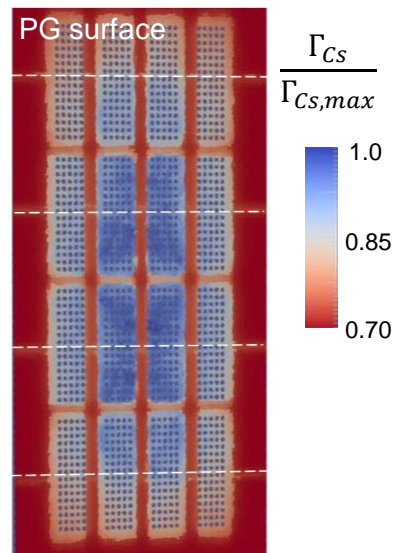
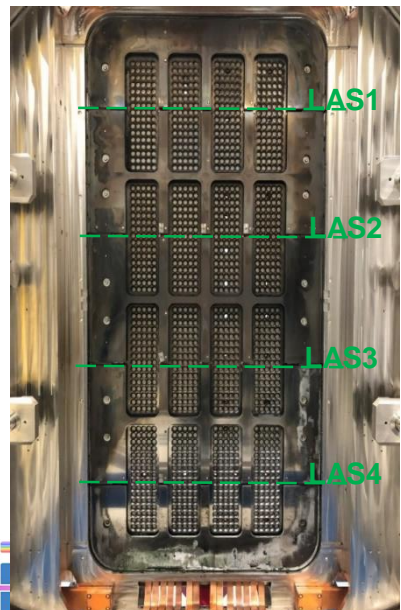
# Control of caesium evaporation and improvement of emission nozzle



Cs IN SWAB ANALYSES OF CIRCULAR STAINS AT EG



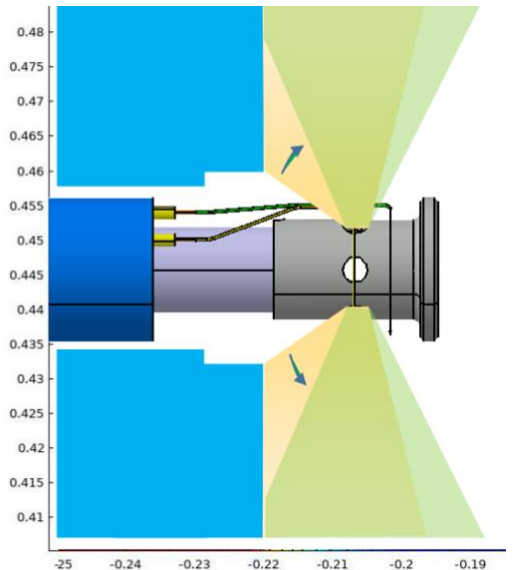
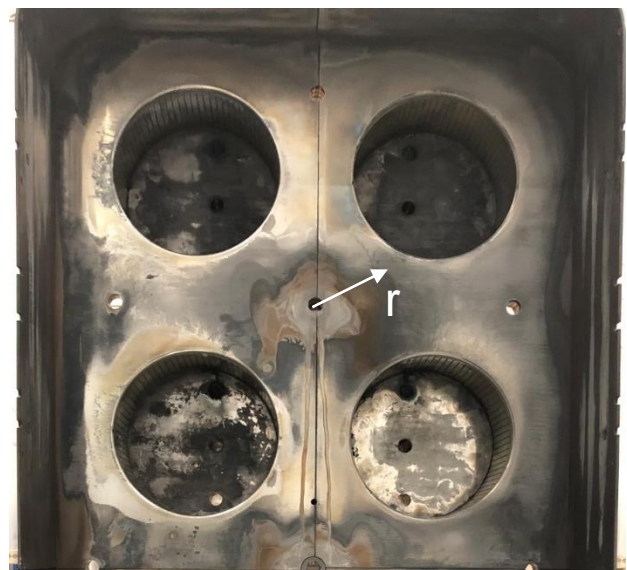
- In SPIDER short-pulse operation with caesium, vacuum phase was key for Cs dynamics: focus on this phase to maximise uniformity
- Comparison of simulations against Laser Absorption Spectroscopy, to verify equal emission from each oven<sup>[1]</sup>
- Comparison against sampling of stains at extraction grid, direct projection through PG apertures of first emission from nozzle<sup>[1],[2]</sup> (not much affected by plasma, nor by stray particles in the accelerator since they are far from the apertures)
- Role of plasma in Cs dynamics: evidence of quite large amount of Cs<sup>+</sup> in the plasma is found at the lateral walls (i.e. maximum amount found at cusps)



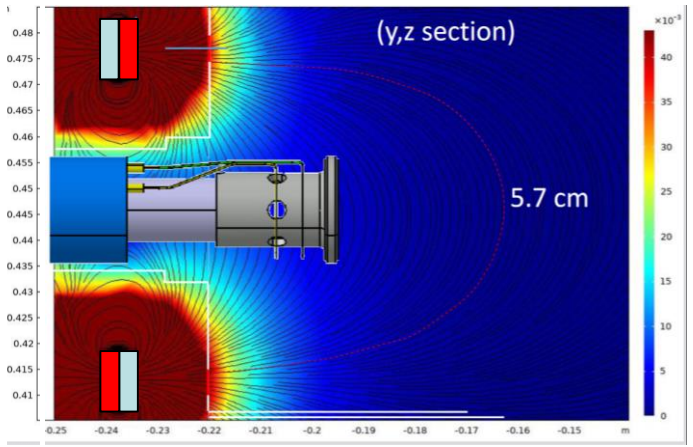
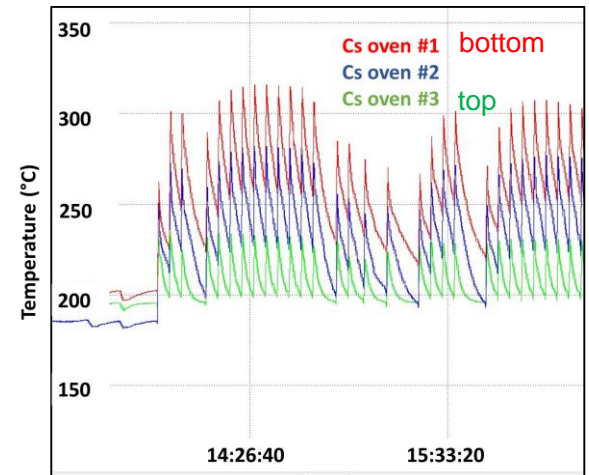
[1] M Fadone, Summary of caesium evaporation and deposition during SPIDER's first campaign, NIBS 2022

[2] M Pavei, Status of SPIDER beam source after the first 3.5 years of operation, SOFT 2022

# Control of caesium evaporation and improvement of emission nozzle



- Oven nozzle geometry shall be improved to avoid evaporating directly around the nozzle

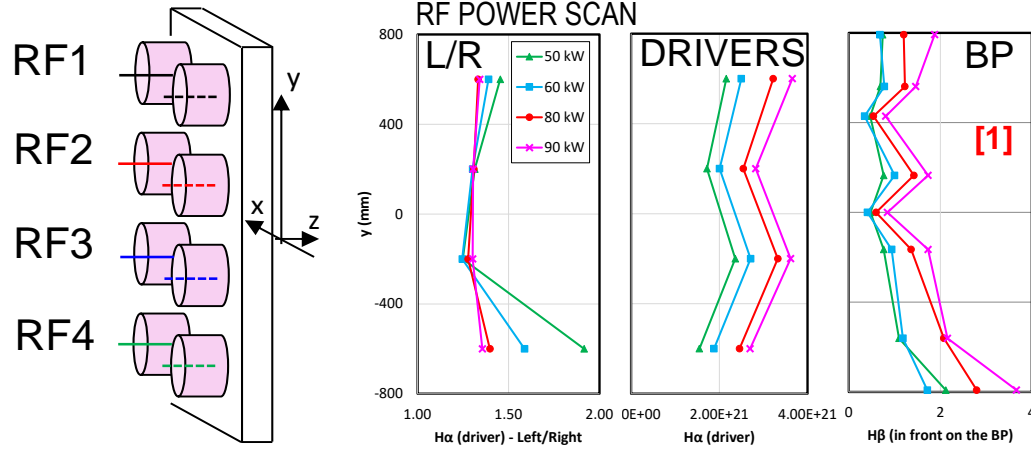


- By interaction with the plasma, the oven nozzles are overheated, each one differently: might result in uncontrolled Cs release (i.e. not in steady-state)

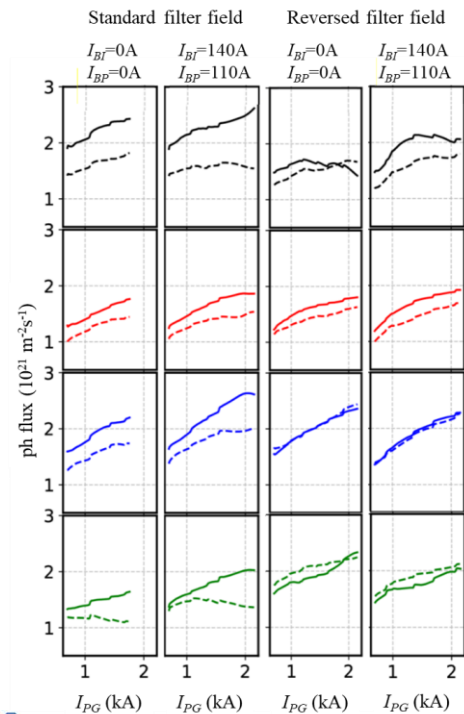
[1] M Fadone, Summary of caesium evaporation and deposition during SPIDER's first campaign, NIBS 2022

[2] M Pavei, Status of SPIDER beam source after the first 3.5 years of operation, SOFT 2022

# Vertical uniformity and non-homogeneities among RF generators

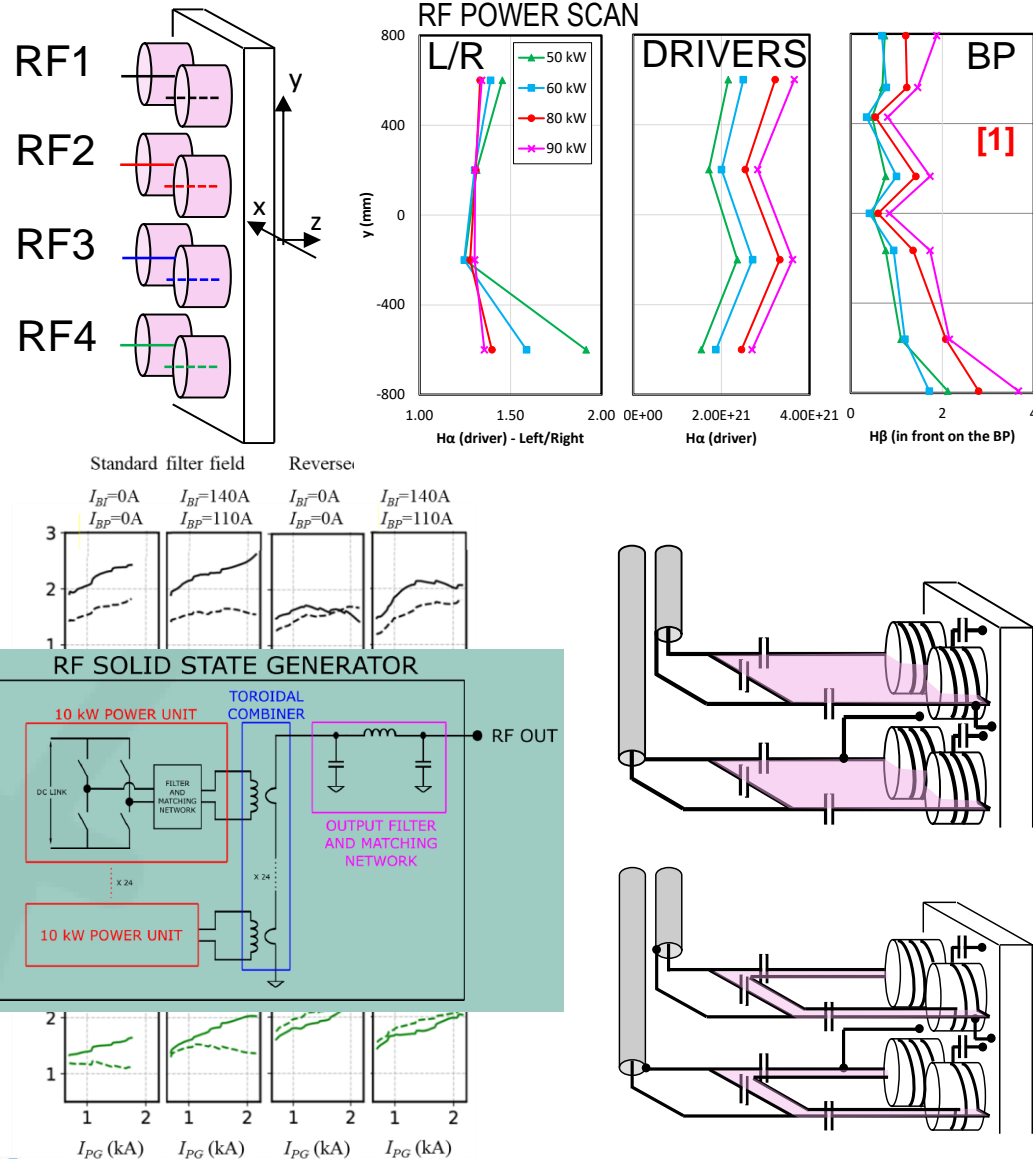


- Beam and plasma parameters along vertical direction depends on RF power, filter field, pressure, bias: difficult to understand link to plasma and source parameters [1],[2]
- Plasma drifts in expansion region mixes with uneven RF power coupled to each driver



[1] M Ugoletti, Study of the relationship between the source complexity and the beam divergence and homogeneity in SPIDER, NIBS 2022  
 [2] M Agostini, Effect of plasma grid and bias plate biasing in SPIDER negative ion beam, NIBS 2022

# Vertical uniformity and non-homogeneities among RF generators



- Beam and plasma parameters along vertical direction depends on RF power, filter field, pressure, bias: difficult to understand link to plasma and source parameters<sup>[1],[2]</sup>
- Plasma drifts in expansion region mixes with uneven RF power coupled to each driver
- Replacement of oscillators with solid-state RF generators<sup>[3],[4],[5]</sup>
  - No internal resonance to set the frequency (avoidance frequency instability), direct control of the frequency allows to reach the best matching → **no output power limitation**
  - Avoidance of cross talk, if driven at the same frequency → **no modulation of RF power** among pairs of drivers
- Optimization of RF circuit geometry to minimise mutual inductance among RF circuits of different generators

[1] M Ugoletti, Study of the relationship between the source complexity and the beam divergence and homogeneity in SPIDER, NIBS 2022

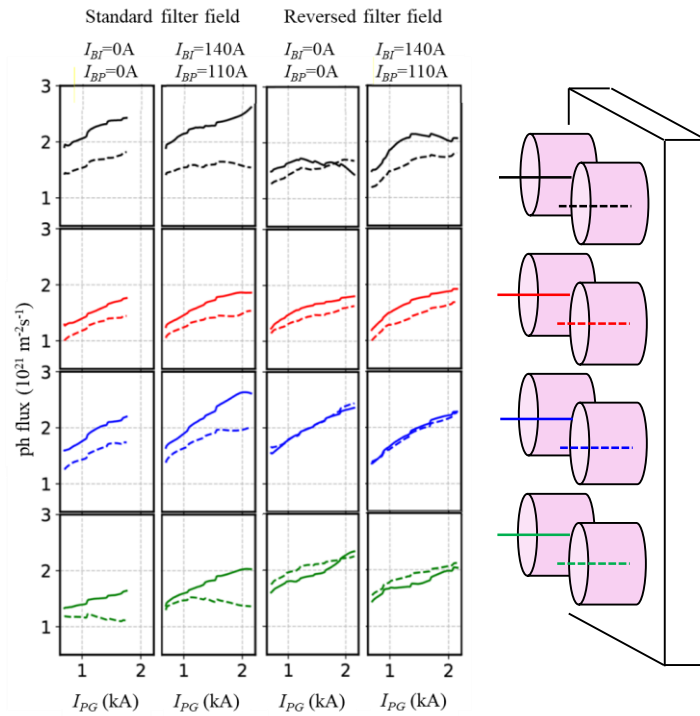
[2] M Agostini, Effect of plasma grid and bias plate biasing in SPIDER negative ion beam, NIBS 2022

[3] A Maistrello, Overview on Electrical Issues Faced During the SPIDER Experimental Campaigns, SOFT 2022

[4] V Toigo, The ITER Neutral Beam Test Facility: status and perspectives , NIBS2022

[5] R Casagrande, Guidelines for the integration of RF solid state generators for the high power ion sources of NBTF experiments and ITER HNB, SOFT 2022

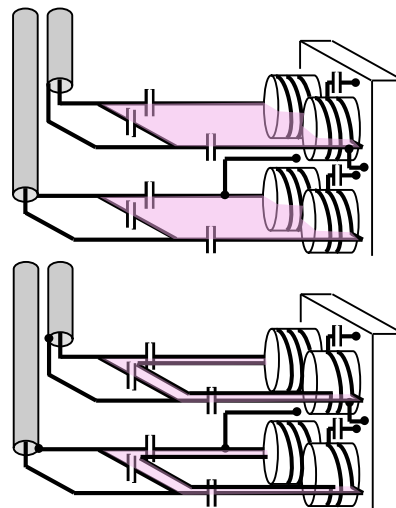
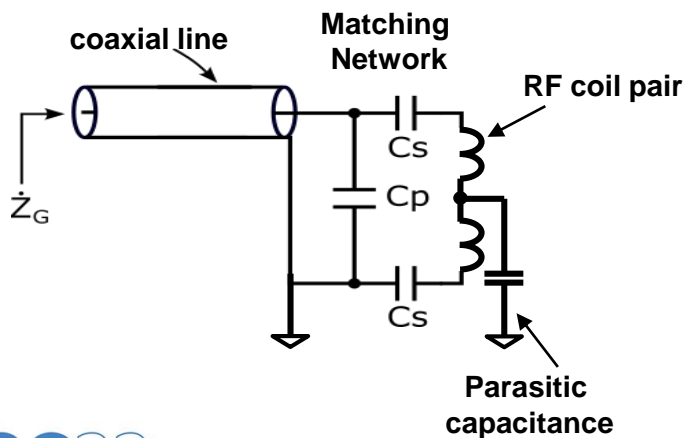
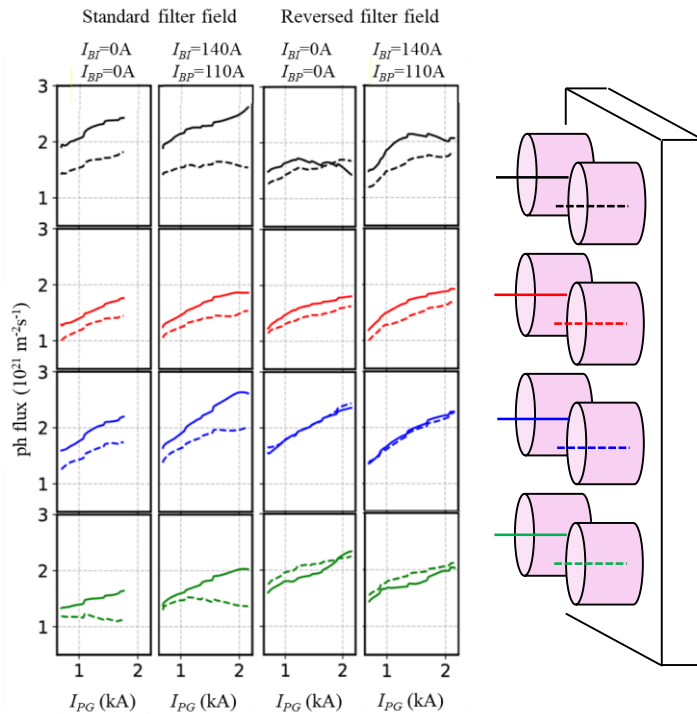
# Left/right symmetry of RF drivers



- Left/right asymmetry depends on filter field and bias. Not easy to justify.



# Left/right symmetry of RF drivers

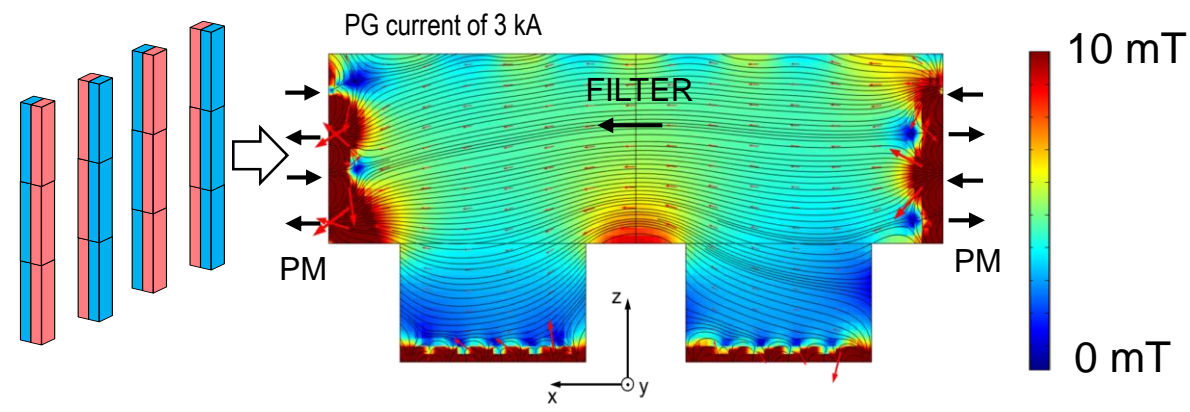


- Left/right asymmetry depends on filter field and bias. Not easy to justify.
- Can be related to RF circuit:
  - asymmetric parasitic capacitance? Difference of the current among RF coil pairs estimated between 2% and 4% (i.e. RF power within 10% difference)
  - Mutual inductance (adding constructively or destructively to its self-induced flux) → minimize mutual inductance, use of solid-state generators will mitigate

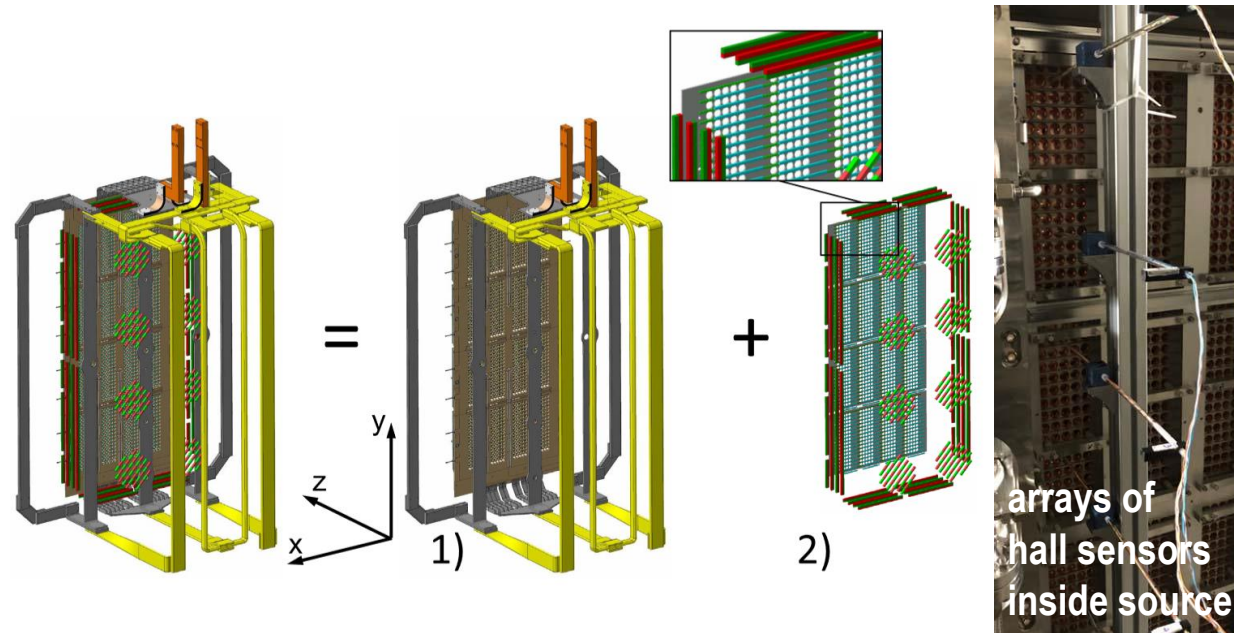
Ongoing analyses to determine plasma parameters from electrical parameters<sup>[1]</sup>

- Can be related to asymmetry of magnetic filter field? Plasma drifts?

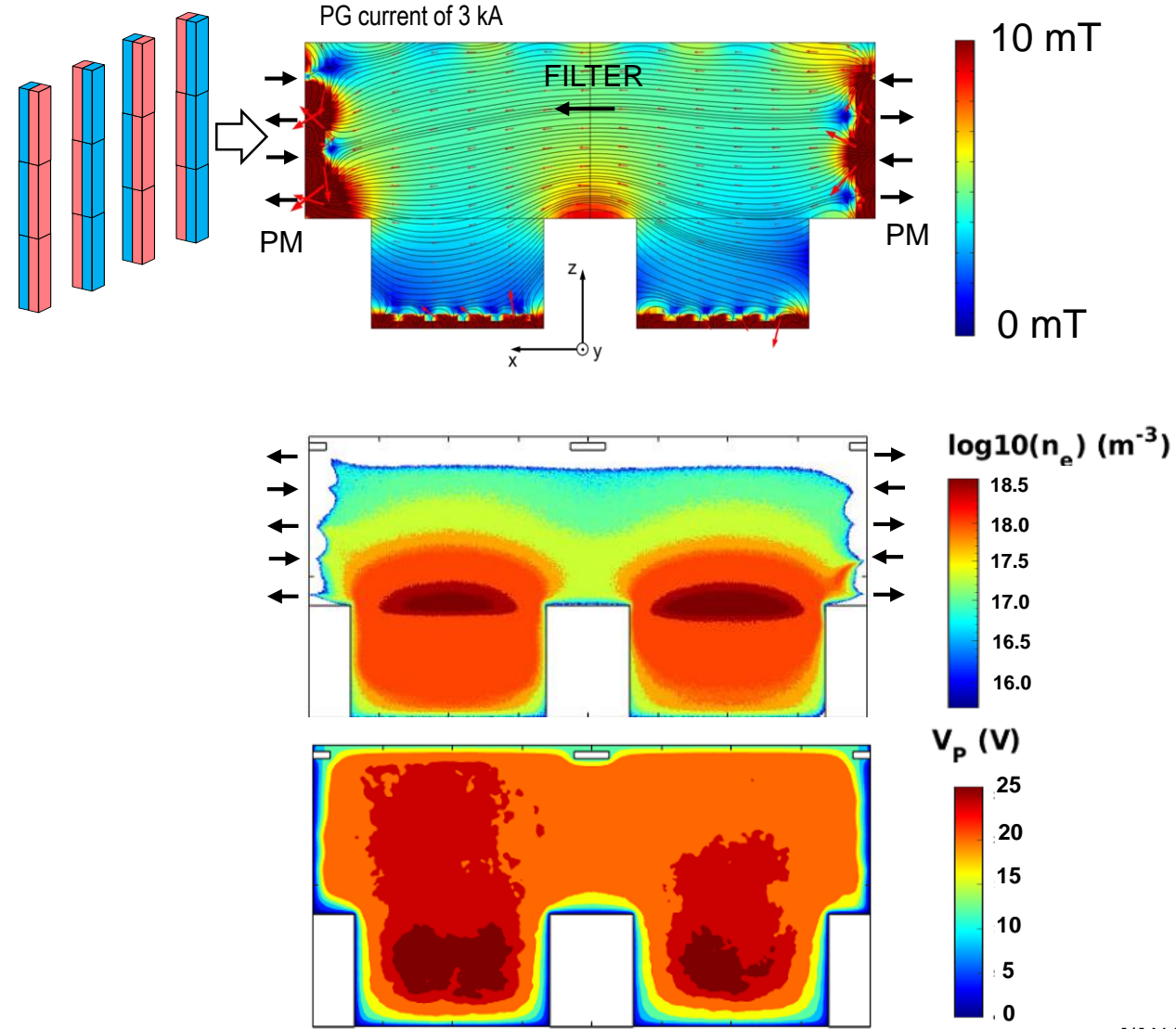
[1] P Jain, Use of electrical measurements for non-invasive estimation of plasma electron density inside the driver of spider, NIBS 2022



- Experimental verification of left/right symmetric contribution from filter field (e.g. unbalanced current on return busbars of PG current) **was verified experimentally**<sup>[1]</sup> (about 10% variation of B strength along vertical direction)
- PM in cusp configuration on lateral walls: left/right asymmetry of B field strength<sup>[1]</sup> (even reaching driver exit plane)

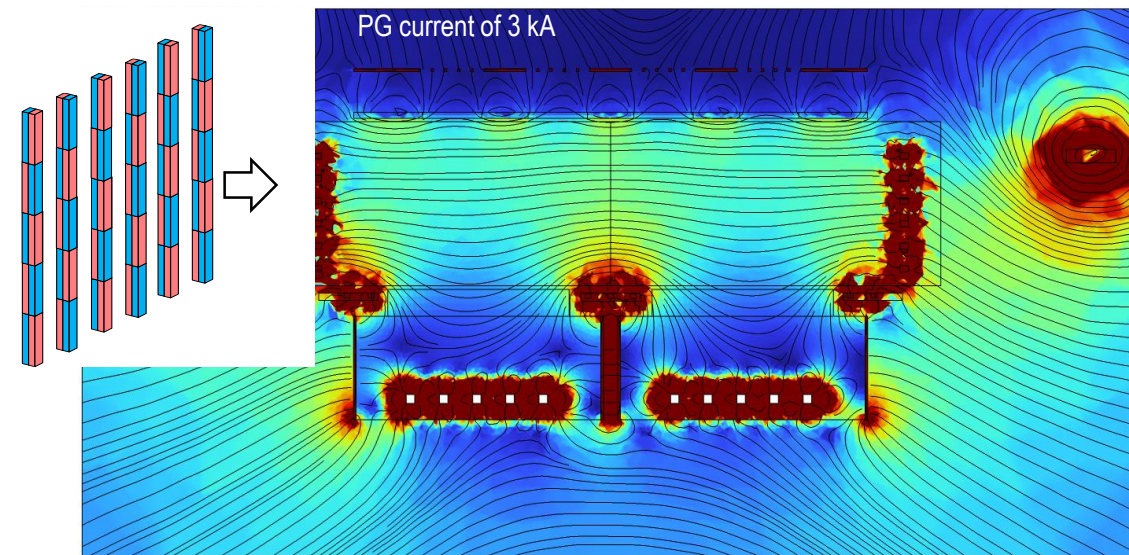
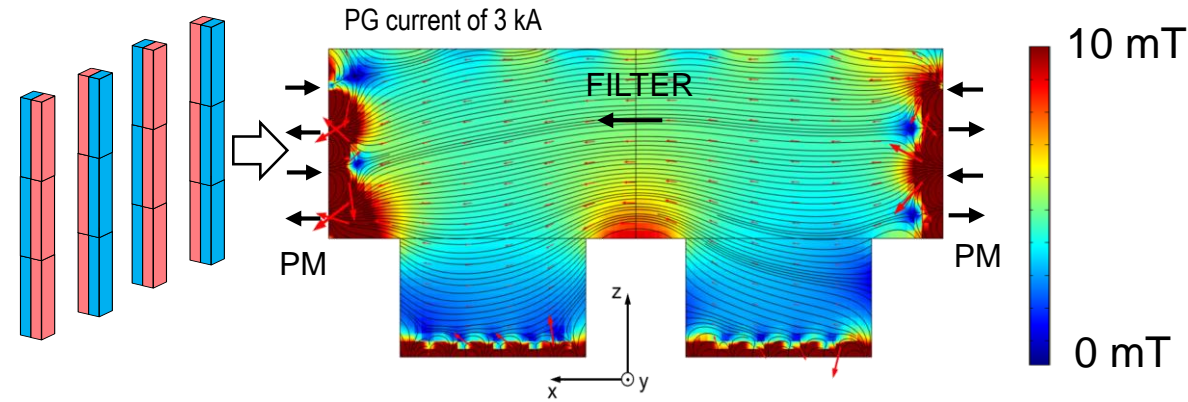


[1] N Marconato, Numerical and experimental assessment of the new magnetic field configuration in SPIDER, IEEE TPS 2022



- Experimental verification of left/right symmetric contribution from filter field (e.g. unbalanced current on return busbars of PG current) was verified experimentally<sup>[1]</sup> (about 10% variation of B strength along vertical direction)
- PM in cusp configuration on lateral walls: left/right asymmetry of B field strength<sup>[1]</sup> (even reaching driver exit plane)
- 2D PIC simulations show the influence of LW magnets on plasma expansion and peak densities (ongoing: simplified filter field for the moment)

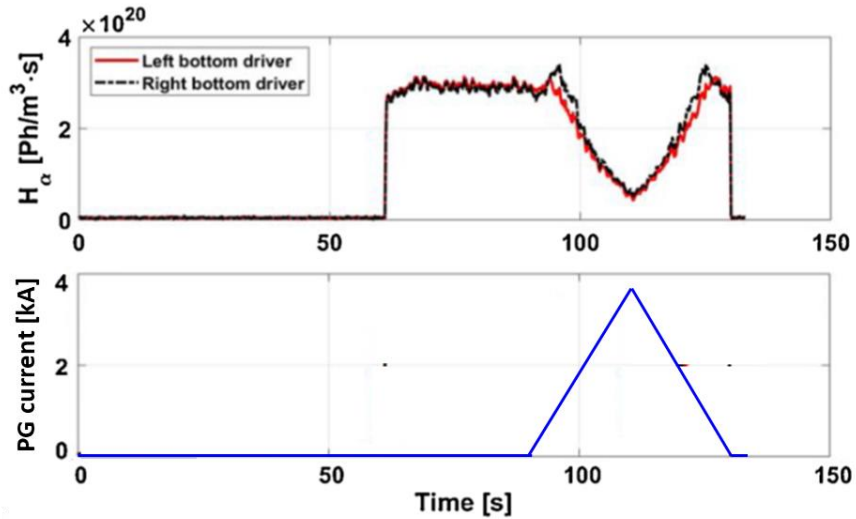
[1] N Marconato, Numerical and experimental assessment of the new magnetic field configuration in SPIDER, IEEE TPS 2022



- Experimental verification of left/right symmetric contribution from filter field (e.g. unbalanced current on return busbars of PG current) was verified experimentally<sup>[1]</sup> (about 10% variation of B strength along vertical direction)
- PM in cusp configuration on lateral walls: left/right asymmetry of B field strength<sup>[1]</sup> (even reaching driver exit plane)
- 2D PIC simulations show the influence of LW magnets on plasma expansion and peak densities
- Change PM volume and cusp configuration at LW to minimise long-range effect<sup>[2]</sup>

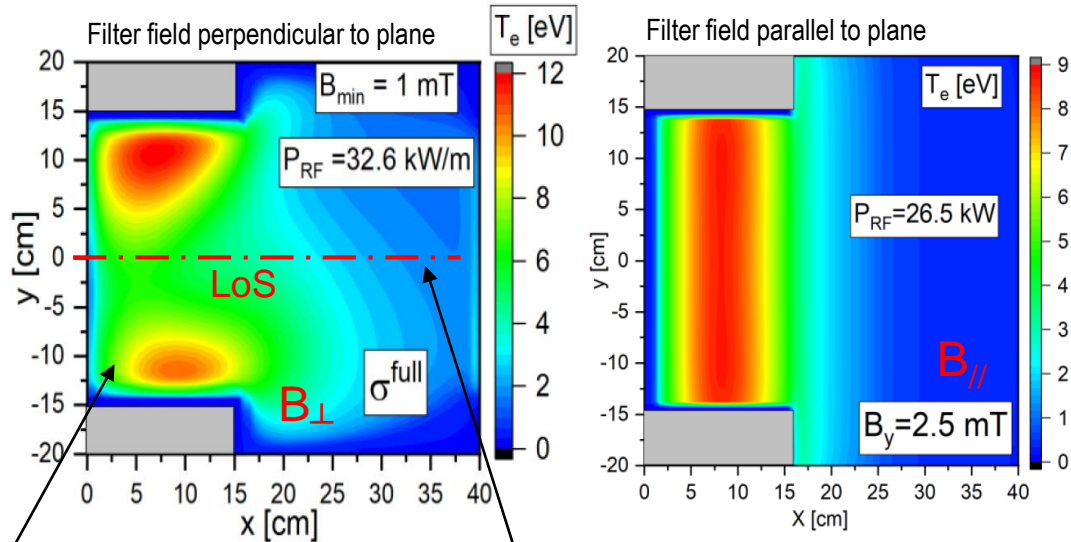
[1] N Marconato, Numerical and experimental assessment of the new magnetic field configuration in SPIDER, IEEE TPS 2022

[2] N Marconato, Integration of new sets of magnets for improved plasma confinement in the SPIDER experiment, SOFT 2022



- In the original configuration, strong transverse filter field strength inside the driver<sup>[1]</sup>. Increasing the filter field turned off the plasma.

[1] N Marconato, An optimized and flexible configuration for the magnetic filter in the SPIDER experiment, FED 166 112281 (2021)



without B field,  $T_e$  always peaks next to the RF coils, whatever the conductivity model;  
with  $B_{\perp}$ , the conductivity model determines the radial profile of absorbed power

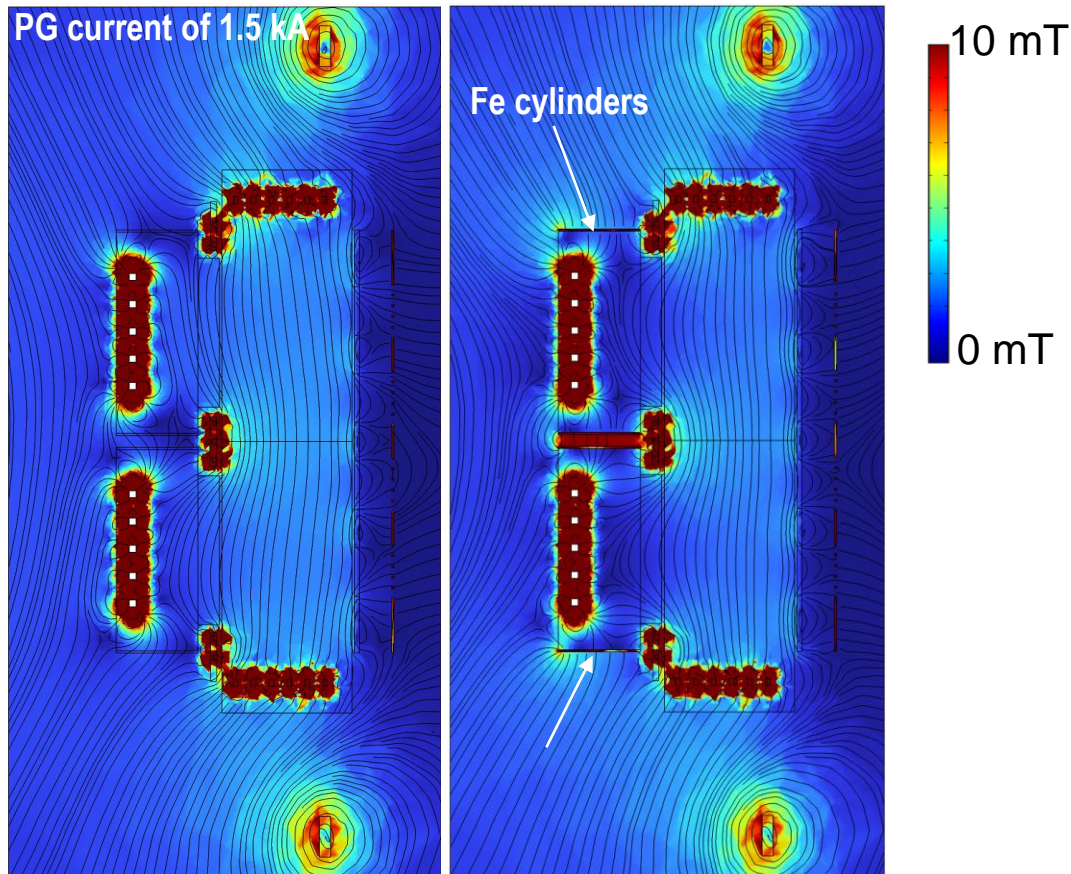
Note that for different field strength, the plasma might move transversally wrt the LoS of the H $\alpha$  signal

- In the original configuration, strong transverse filter field strength inside the driver<sup>[1]</sup>. Increasing the filter field turned off the plasma
- 2D steady-state fluid model FSFS2D (Fluid Solver For SPIDER in 2D)<sup>[2]</sup>. Fluid equations weakly coupled ( $P_{RF}$  and conductivity  $\sigma$ ) to complex  $E_{\theta}$  induced field<sup>[3]</sup> (cylindrical symmetry, harmonic current, no displacement current)

$$\partial_r(r\partial_r E_{\theta}^p) + r\partial_{xx} E_{\theta}^p - \frac{E_{\theta}^p}{r} - i\omega r\mu_0\sigma E_{\theta}^p = i\omega r\mu_0\sigma E_{\theta}^v$$

- In  $B_{\perp}$  simulation, filter field strength is beneficial for confinement;  $B_{//}$  simulation however provides possible explanation for experimental behavior (note that cylindrical approximation is not valid, intrinsically 3D)
- Experimental measurements showed lower  $T_e$  next to the faraday shield, higher at center  $\rightarrow$   $B_{//}$  simulation might provide (partial) explanation

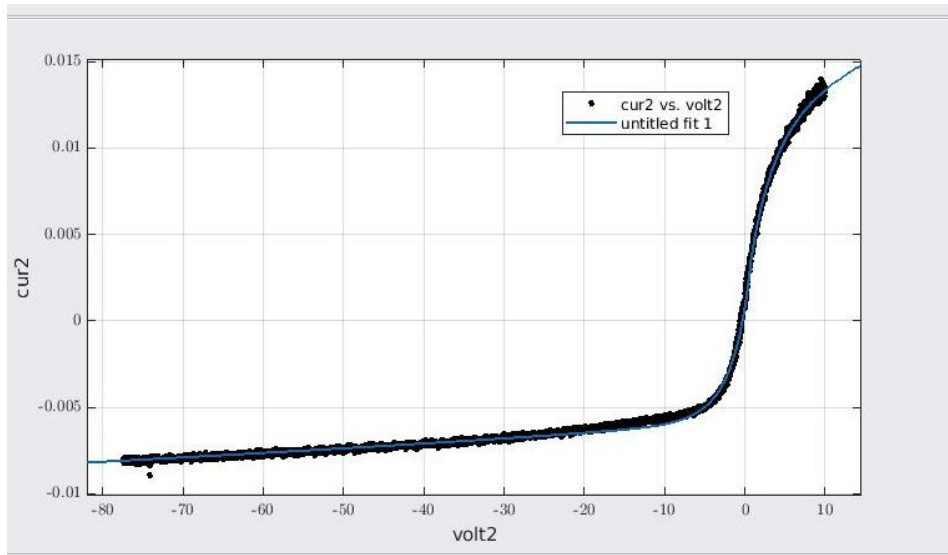
[1] N Marconato, An optimized and flexible configuration for the magnetic filter in the SPIDER experiment, FED 166 112281 (2021)  
[2] R Zagórski, 2-D Fluid Model for Discharge Analysis of the RF-Driven Prototype Ion Source for ITER NBI (SPIDER), IEEE TPS 2022  
[3] R Zagórski, 2D simulations of inductive RF heating in the drivers of the SPIDER device, SOFT 2022



- In the original configuration, strong transverse filter field strength inside the driver<sup>[1]</sup>. Increasing the filter field turned off the plasma
- Use of ferromagnetic cylinders (e.g. outside the electromagnetic shields of RF drivers) is one option to minimise the filter field inside drivers<sup>[4]</sup> (up to driver's exit, about 1/2 of the original value) Inside the drivers it now is reduced to about 30% of the value in the expansion region (it is about 65% without Fe).

[4] N Marconato, Integration of new sets of magnets for improved plasma confinement in the SPIDER experiment, SOFT 2022

# Preparing future investigation of nonuniformities from drivers to extraction region



- Model for the analysis of current-voltage characteristics of embedded langmuir probes in highly electronegative plasma<sup>[1]</sup>
- Optimization of optical emission spectroscopy and collisional-radiative models for its interpretation<sup>[2],[3]</sup>

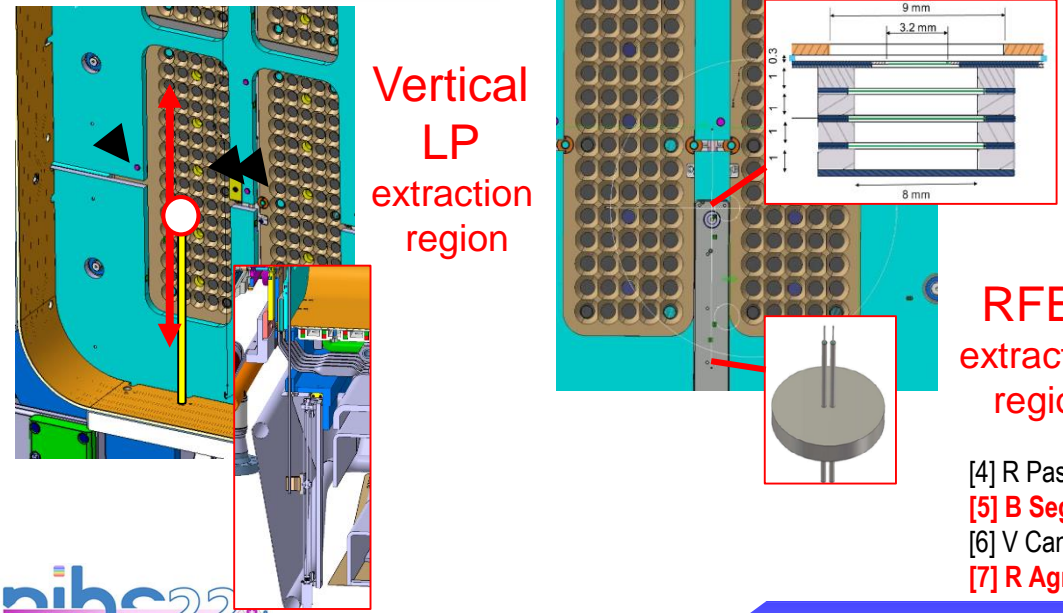
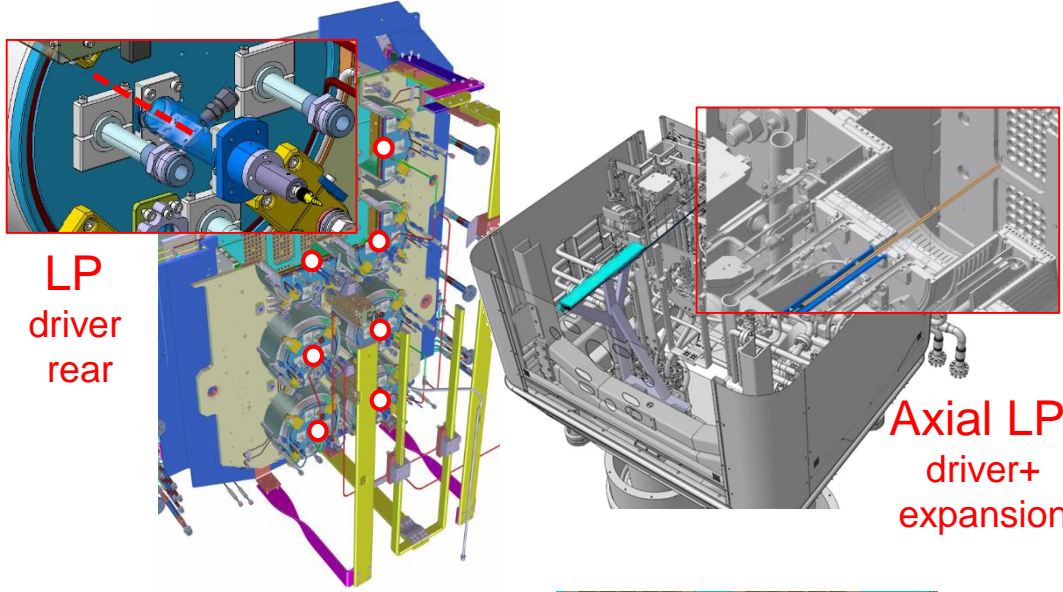
[1] C Poggi, Highly electronegative plasma conditions in the SPIDER negative ion source, NIBS 2022

[2] D Bruno, Rotational and vibrational temperatures of Hydrogen nonequilibrium plasmas from Fulcher band emission spectra, NIBS2022

[3] I Mario, Plasma emission monitored via optical emission spectroscopy during the Cs conditioning at SPIDER, NIBS 2022



# Preparing future investigation of nonuniformities from drivers to extraction region



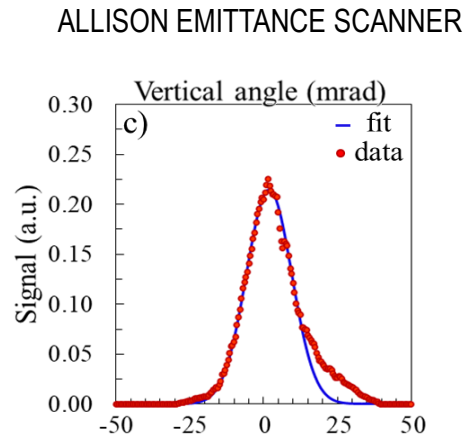
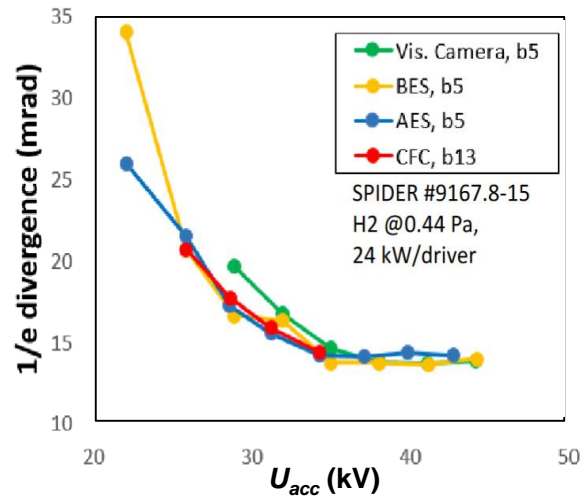
- Model for the analysis of current-voltage characteristics of embedded langmuir probes in highly electronegative plasma<sup>[1]</sup>
- Optimization of optical emission spectroscopy and collisional-radiative models for its interpretation<sup>[2],[3]</sup>
- vertical profiles in the plasma within beamletgroup: movable Langmuir probe at the extraction<sup>[4]</sup>, also compatible with the use of Cavity-Ring-Down laser for photodetachment<sup>[5]</sup>
- Compact Retarding Field Energy analyser on the Bias Plate<sup>[5]</sup>
- Fast axial movable Langmuir probe, to assess also during caesiation the plasma parameters along the driver axis and hte expansion region<sup>[6]</sup>
- Role of electrons fundamental: feasibility study for an interferometer<sup>[7]</sup>, and of a cut-off probe<sup>[5]</sup> for measurement of the electron density

[4] R Pasqualotto, Improvement of SPIDER diagnostic systems, SOFT 2022

[5] B Segalini, Study and development of diagnostic systems to characterise the extraction region in SPIDER, NIBS 2022

[6] V Candeloro, Design of a movable electrostatic diagnostic for the investigation of plasma prop. in a large neg. ion source SOFT 2022

[7] R Agnello, Numerical and experimental investigations of a microwave interferometer for the negative ion source SPIDER, NIBS 2022

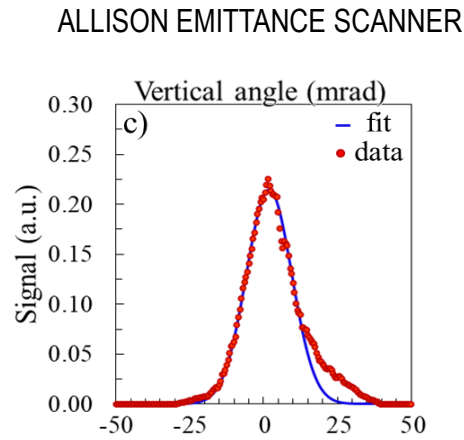
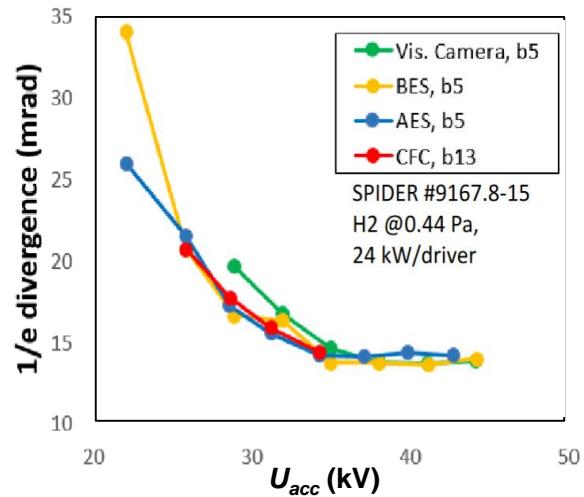


- Study of single beamlet optics in SPIDER important in view of ITER HNB, measurement of angular distribution<sup>[1]</sup> and confirm required divergence (transmission to ITER & possibility of beam halo interception by accelerator grids)
- Beam divergence in SPIDER can be measured by four diagnostics, good agreement among them, in general not better than 12 mrad<sup>[2]</sup>

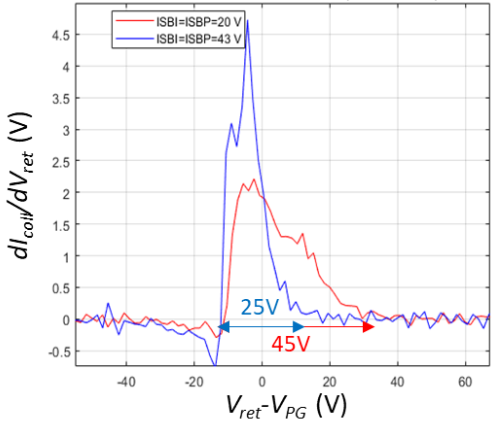
[1] G Serianni, SOFE2021, IEEE-Trans Plasma Sci. (2022)

[2] P Veltri, Towards low divergence beams for the ITER neutral beam injection system, NIBS 2022

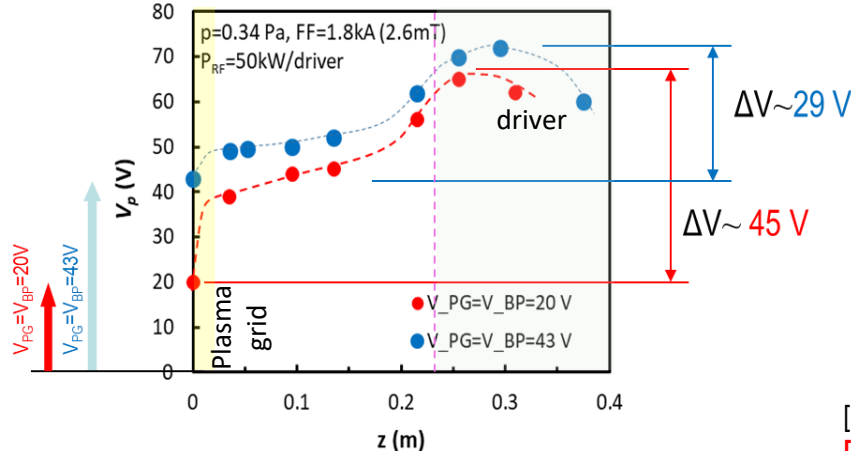
# Beamlet optics and possible improvements



RETARDING FIELD ENERGY ANALYSER  
P=0.34 Pa, FF=2kA (3.2mT), D2



PLASMA POTENTIAL FROM MOVABLE LANGMUIR PROBES



- Study of single beamlet optics in SPIDER important in view of ITER HNB, measurement of angular distribution<sup>[1]</sup> and confirm required divergence (transmission to ITER & possibility of beam halo interception by accelerator grids)
- Beam divergence in SPIDER can be measured by four diagnostics, good agreement among them, in general not better than 12 mrad<sup>[2]</sup>
- Possible approach for improving divergence:
  - Reduce energy of H<sup>-</sup> precursors
  - Increase positive ion density, while diminishing the energy source for positive ions<sup>[3]</sup>
- Reducing plasma potential would additionally diminish driving forces for vertical drifts

[1] G Serianni, SOFE2021, IEEE-Trans Plasma Sci. (2022)

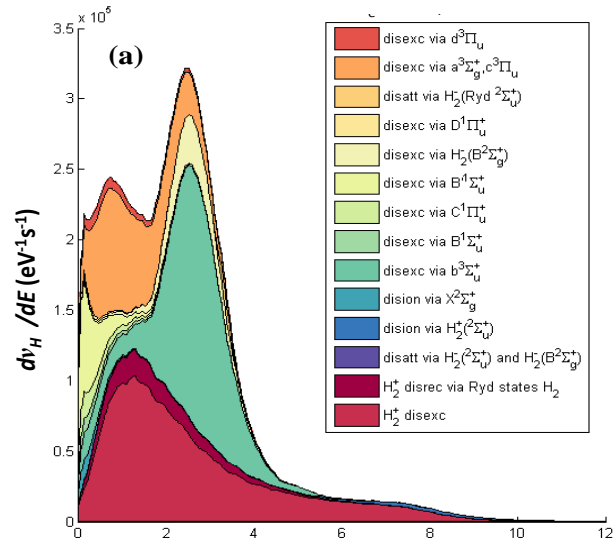
[2] P Veltri, Towards low divergence beams for the ITER neutral beam injection system, NIBS 2022

[3] A Pimazzoni, Key parameters for the ion velocity distribution at the plasma meniscus of a caesiated negative ion source, NIBS 2022

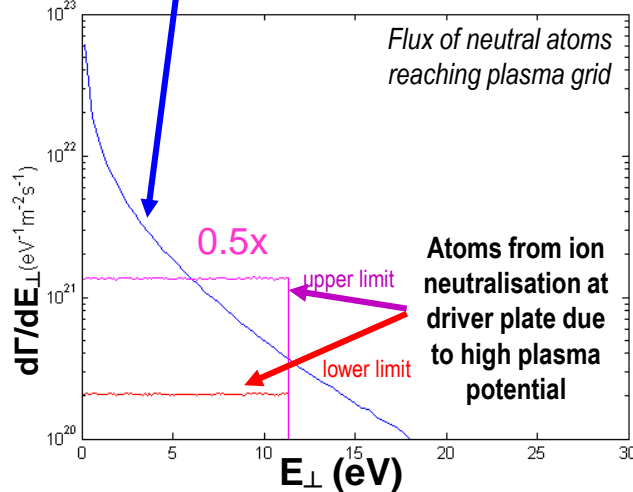
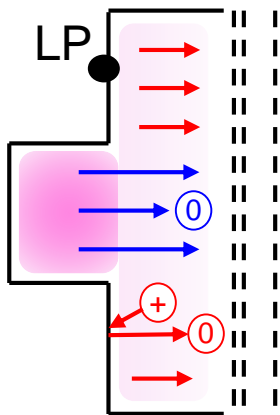
# Hot atoms and plasma loss at rear walls



Kinetic Energy Release of dissociation  $H^0$  fragments,  $T_e=15$  eV,  $n_e=3 \times 10^{18} \text{ m}^{-3}$



Atoms from dissociation inside  $E$  (eV)  
RF drivers ( $1.5 \times 10^{18} \text{ m}^{-3}$ ),  
isotropic distribution

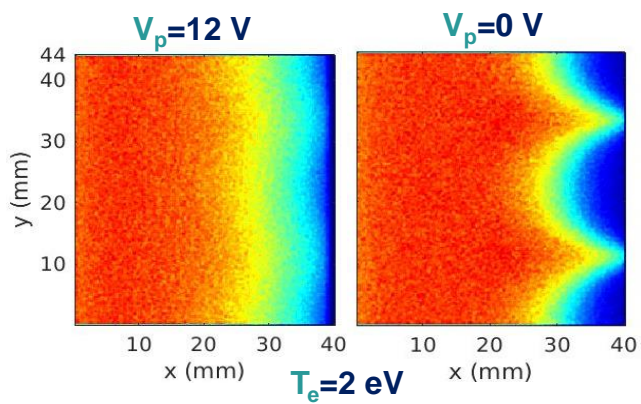
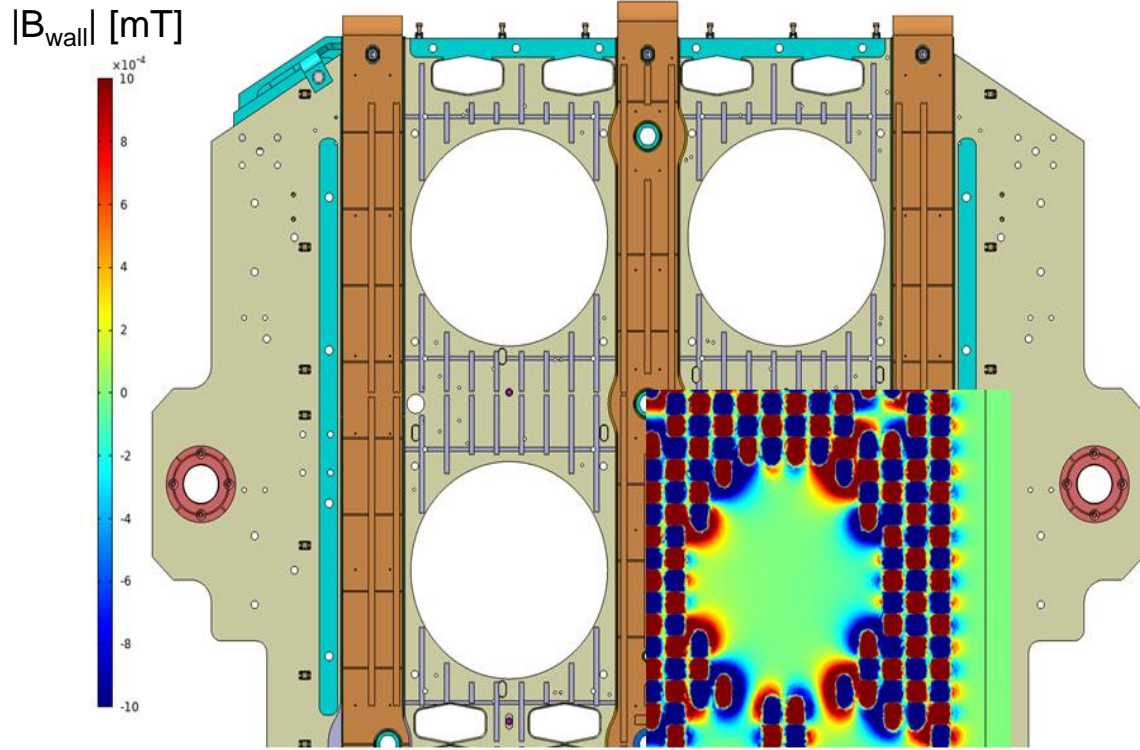


- Numerical simulation of energy distribution of atoms generated by dissociation inside ion source<sup>[1]</sup>
- Measurement of plasma parameter before plasma driver plate (i.e. rear wall of expansion chamber)<sup>[2]</sup>
- Ion neutralisation at rear walls<sup>[3]</sup> causes high-energy tail of hot atom reaching Plasma Grid

[1] E Sartori, Energy distribution of fragments in dissociation by electron impact for the use in numerical models applied to negative ion sources, NIBS 2022

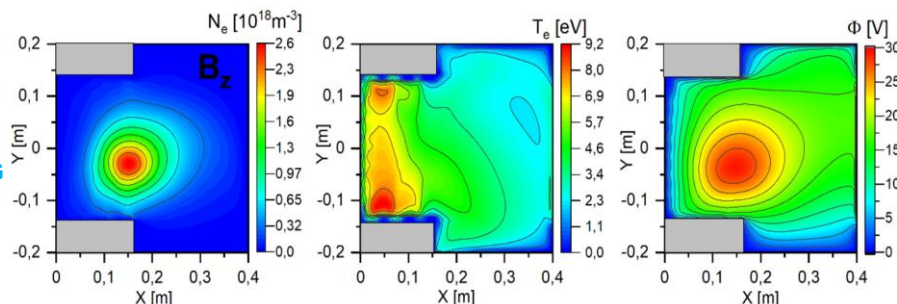
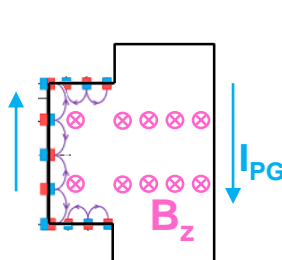
[2] V Candeloro, Development of a Triple Langmuir Probe for Plasma Characterization in SPIDER, IEEE TPS

[3] G Fubiani, New Journal of Physics 015002, 2017

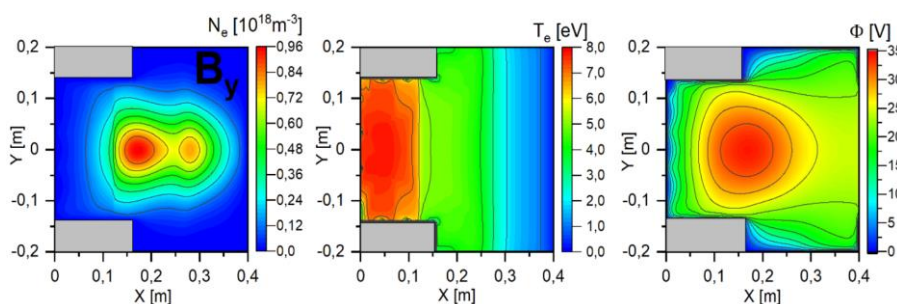
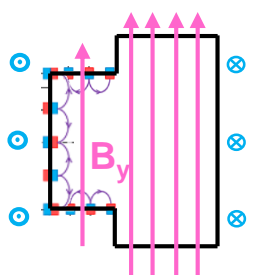


- Numerical simulation of energy distribution of atoms generated by dissociation inside ion source<sup>[1]</sup>
- Measurement of plasma parameter before plasma driver plate (i.e. rear wall of expansion chamber)<sup>[2]</sup>
- Ion neutralisation at rear walls<sup>[3]</sup> causes high-energy tail of hot atom reaching Plasma Grid
- Importance of rear walls on the overall plasma loss: quite important reduction of total ion losses (not ambipolar) expected from analytical estimation (about -20%)
- Study of multicusp effectiveness<sup>[5]</sup> with  $V_p > V_{\text{floating}}$  (typical of lateral wall and rear wall of expansion region)

[1] E Sartori, Energy distribution of fragments in dissociation by electron impact for the use in numerical models applied to negative ion sources, NIBS 2022  
[2] V Candeloro, Development of a Triple Langmuir Probe for Plasma Characterization in SPIDER, IEEE TPS  
[3] G Fubiani, New Journal of Physics 015002, 2017  
[4] N Marconato, Integration of new sets of magnets for improved plasma confinement in the SPIDER experiment, SOFT 2022  
[5] V Candeloro, Influence of plasma parameters on the effectiveness of multi-cusp magnetic field confinement in negative ion sources, NIBS 2022



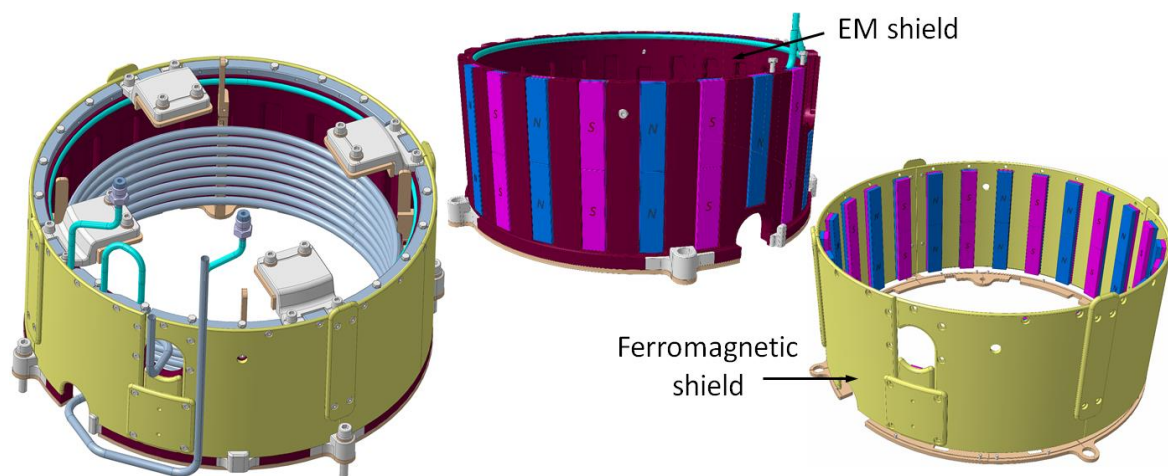
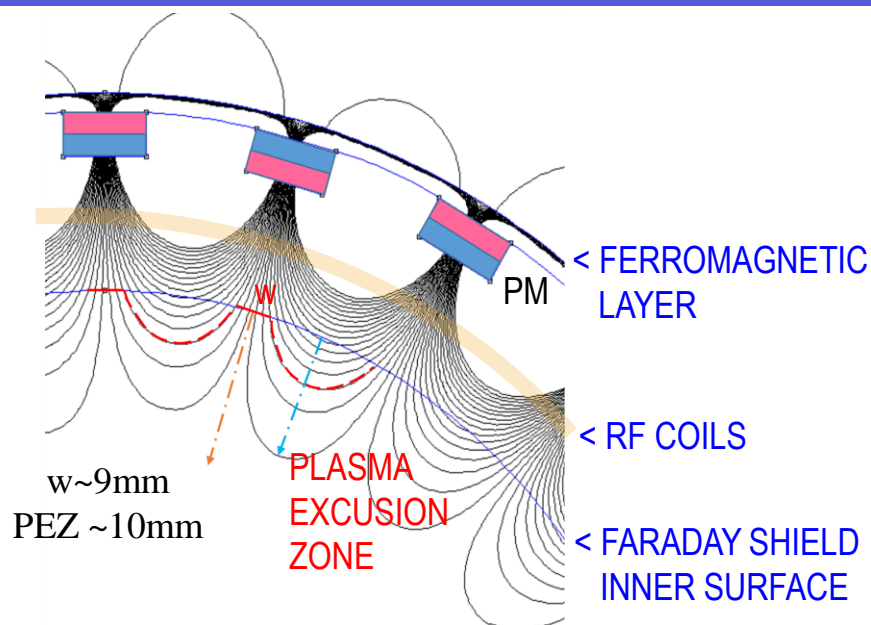
wrt case without magnets: +150%  $n_e$ , -25%  $T_e$ , -20%  $V_p$



30 kW,  $B_{\perp}(x)$  from 1mT to 2mT, depleted  $n_{H_2}$  2.5 to  $4.5 \times 10^{19} \text{ m}^{-3}$   
 wrt case without magnets: +60%  $n_e$ , -40%  $T_e$ , -22%  $V_p$

- Aim: increasing plasma density and reducing plasma potential via multicusp confinement
- In the absence of 3D models: 2D fluid simulations<sup>[1]</sup> on planes perpendicular rather than parallel to B yield.  $n_e \uparrow$ ,  $V_p \downarrow$

[1] R Zagorski, Influence of different magnetic configurations on plasma parameters in SPIDER device, NIBS 2022

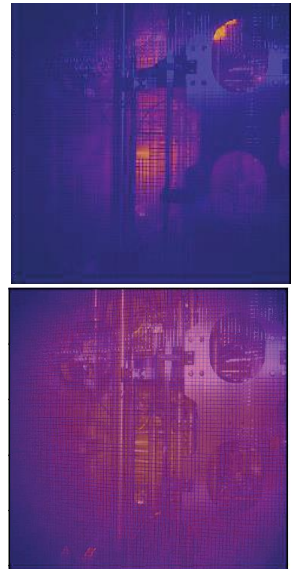
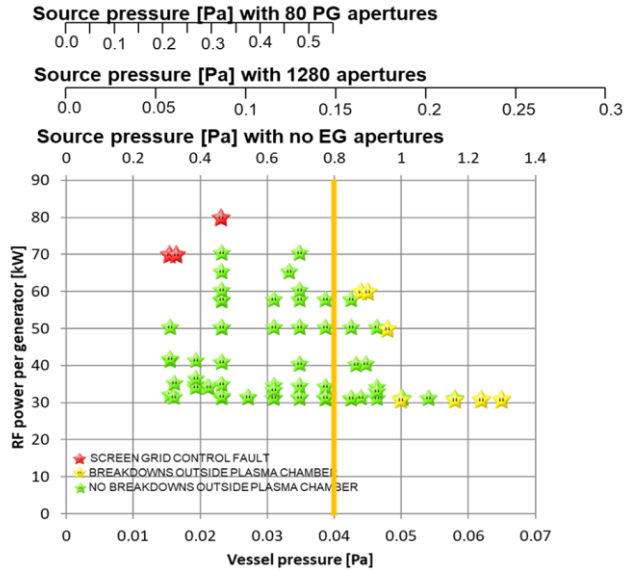


- Aim: increasing plasma density and reducing plasma potential via multicusp confinement
- In the absence of 3D models: 2D fluid simulations<sup>[1]</sup> on planes perpendicular rather than parallel to B yield.  $n_e \uparrow$ ,  $V_p \downarrow$
- Implementation in cylindrical coordinates<sup>[2]</sup> exploits the possibility to install ferromagnetic layer outside
- First order figure of merit: increase of plasma density (thanks to reduced leak width w) times decrease of plasma volume (due to plasma excision zones)  $\sim 3.5x$

[1] R Zagorski, Influence of different magnetic configurations on plasma parameters in SPIDER device, NIBS 2022

[2] N Marconato, Integration of new sets of magnets for improved plasma confinement in the SPIDER experiment, SOFT2022

# SPIDER Operating scenarios with improved pumping system



- vessel pressure limited by breakdowns on rear side of RF source (when operating multiple RF generators)
- Improved pumping system based on NEG: pumping speed of one cartridge based on characterisation at KIT, taken at RT and 0.2 Torr L/g of H<sub>2</sub> concentration (i.e. beginning of gas injection; of at 4.7 Torr L/g, it is about 25% lower)



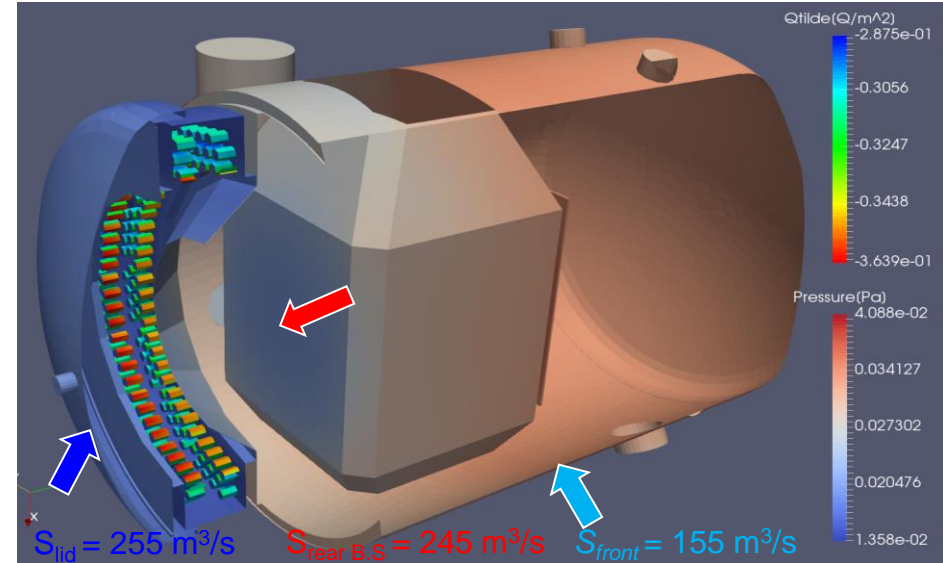
[1] M. Pavei, et al., Fus Eng Des 161 (2020) 112036  
 [2] S Hanke, Experimental characterisation of a large NEG pump towards its application in DEMO neutral beam injectors, SOFT 2022  
 [3] M Siragusa, SPIDER Vacuum Enhancement: a NEG-pump based project, presented AIV conference 2022



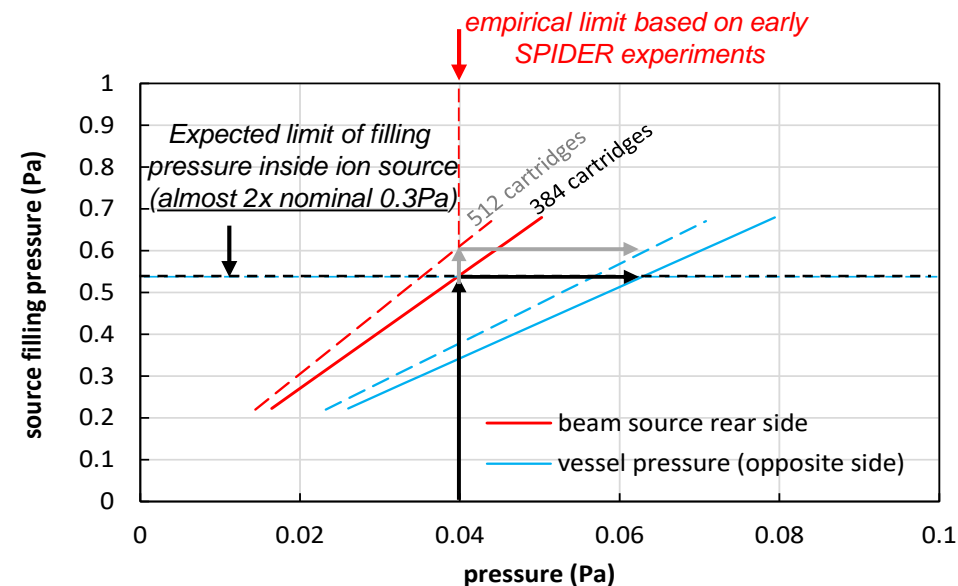
# SPIDER Operating scenarios with improved pumping system



Source filling pressure  $\rho_{source}=0.283$  Pa  
 4+2 TMPs (13.5 m<sup>3</sup>/s), 8 cryo (80 m<sup>3</sup>/s),  
 384 NEG cartridges (0.87 m<sup>3</sup>/s each)



- vessel pressure limited by breakdowns on rear side of RF source (when operating multiple RF generators)
- Improved pumping system based on NEG: pumping speed of one cartridge based on characterisation at KIT, taken at RT and 0.2 Torr L/g of H<sub>2</sub> concentration (i.e. beginning of gas injection; of at 4.7 Torr L/g, it is about 25% lower)
- 3D simulations show the ratio expected for source pressure vs vessel pressure (with all 1280 apertures, almost 0.6 Pa filling pressure is possible) and gas load on each cartridge (uniform within 5%)

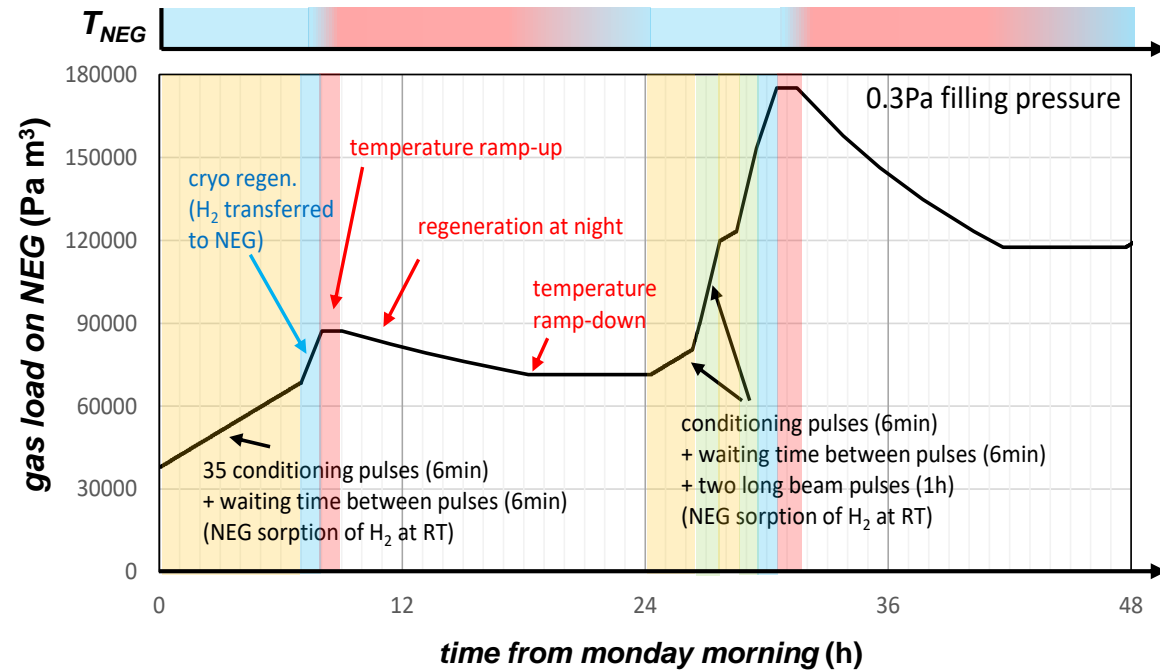


[1] M. Pavei, et al., Fus Eng Des 161 (2020) 112036

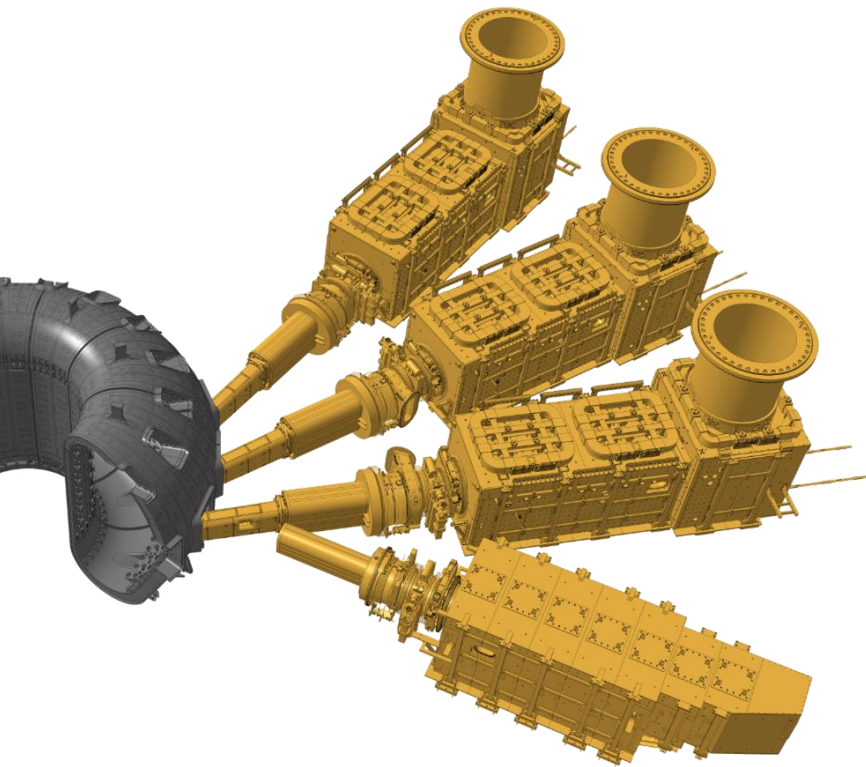
[2] S Hanke, Experimental characterisation of a large NEG pump towards its application in DEMO neutral beam injectors, SOFT 2022

[3] M Siragusa, SPIDER Vacuum Enhancement: a NEG-pump based project, presented AIV conference 2022

# SPIDER Operating scenarios with improved pumping system



- vessel pressure limited by breakdowns on rear side of RF source (when operating multiple RF generators)
- Improved pumping system based on NEG: pumping speed of one cartridge based on characterisation at KIT, taken at RT and 0.2 Torr L/g of H<sub>2</sub> concentration (i.e. beginning of gas injection; of at 4.7 Torr L/g, it is about 25% lower)
- 3D simulations show the ratio expected for source pressure vs vessel pressure (with all 1280 apertures, almost 0.6 Pa filling pressure is possible)
- Operating scenario with NEG pumping at RT (for NEG protection in case of water leak, investment protection level)
  - Pumping speed vs hydrogen load curve
  - Effect of background gas over time (H<sub>2</sub>O, outgassing, minor leaks) slowly decrease the NEG performance, independently of hydrogen load → performance fully restored by short reactivation cycles at night
  - Long regeneration during weekends
- Cryogenic pumps and turbopumps operate in parallel, and deal with non-getterable gases → hydrogen load transferred to NEG at the end of every day



- SPIDER results are in line with smaller RF sources, of similar design
- Experience of first 3.5y of SPIDER operation: we studied beam and plasma performances to anticipate as much as possible future issues
  - Nonuniformities of extracted current density on the unexpected scale of beamlet group
  - High divergence and presence of tails in the angular distribution
- After the present shutdown, we should be in the conditions to really assess the performances of the full-scale ITER source!
- In view of the future operations of ITER HNB, the study and test of solutions to decrease divergence and to mitigate non-uniformities shall start ASAP